

**AN EXPLORATION INTO RINGS OF OSCILLATORS
USING THE RICKER MODEL**

A Thesis

Presented to the

Faculty of

California State Polytechnic University, Pomona

In Partial Fulfillment

Of the Requirements for the Degree

Master of Science

In

Mathematics

By

Hung Doan

2020

SIGNATURE PAGE

THESIS: AN EXPLORATION INTO RINGS OF OSCILLATORS
USING THE RICKER MODEL

AUTHOR: Hung Doan

DATE SUBMITTED: Spring 2020

Department of Mathematics and Statistics

Dr. Hubertus F. von Bremen
Thesis Committee Chair
Mathematics & Statistics

Dr. Alan Krinik
Mathematics & Statistics

Dr. Jennifer M. Switkes
Mathematics & Statistics

ACKNOWLEDGMENTS

I would like to thank Dr. von Bremen for his support throughout this thesis. There were many times when you believed in me, even when I did not believe in myself. Your vast knowledge is truly an inspiration as I continue my journey in industry. Thank you for all the advice you gave me, both in mathematics and in life. I would also like to thank Dr. Switkes and Dr. Krinik. Both of you have a true passion for teaching and for your students and I am very grateful to have you on my committee. To my parents, I hope you know I did this for you. It was because of you that any of this was possible. To my grandma, you have taught me so much and have supported me every step of the way. To my siblings, Eden, Evan, and Emily, you guys pick up more of my slack than you know. To my coaches/second parents, Glen and Betty, thank you for teaching me hard work and dedication. I will always remember all of the adventures you took me on. To my best friend, Bronson, I wouldn't have even studied mathematics if not for you. To Terry, Chuck and Quincy, you guys have been there for me throughout the Navy and are still there for me now. To Miguel, Steven and Randy, you guys have always pushed me to do better. To my classmates, Sam, Tommy, Darian, Erin and Adrian, I can't imagine doing this Master's without you. And finally, to Angie, you supported me so much and I will always be grateful.

ABSTRACT

In this paper, we explore the response of homogeneous and non-homogeneous rings of oscillators using the Ricker model. We begin in chapter two by introducing the Ricker model and its bifurcation plot. We observe regions of the bifurcation plot for which we obtain periodic solutions and other regions for which we obtain chaotic solutions. Whether a response is periodic or chaotic can be determined by its Lyapunov Characteristic Exponent (LCE), which is discussed in chapter three. In chapter four, we observe the evolution of a single node and see how the system can spontaneously change from an apparant chaotic response to a periodic response. We find that, when acting independently, these oscillators display a chaotic response for given values of the intrinsic growth rate. However, when connecting these oscillators to their nearest neighbors, the response becomes periodic. We then observe the dynamical behavior of connected rings of oscillators by changing the initial conditions. We explore symmetric node responses where we find that the projection of node values can be the same when reflected about an oscillator. We vary the values of system parameters such as the connection strength to each node and the number of connected nodes in a ring, and determine for which of these values result in periodic solutions. In chapter five, we explore a ring of non-identical oscillators. By plotting LCEs for varying values of the connection strength, we find that the global response of non-homogeneous rings is complex. Lastly, in chapter six, we explore the dynamical behavior of coupling rings of non-homogeneous oscillators. The work in this paper parallels the work done by Hubertus von Bremen in [1]; here we focus exclusively on the Ricker model.

Contents

Signature Page	ii
Acknowledgements	iii
Abstract	iv
List of Figures	viii
List of Tables	ix
Chapter 1 Introduction	1
Chapter 2 The Ricker Model	5
Chapter 3 Lyapunov Characteristic Exponents	8
Chapter 4 A ring of identical oscillators	11
4.1 Evolution of a single node	12
4.2 Effect of changing the seed value	17
4.3 Symmetric node responses	20
4.4 Effect of changing the connection strength	22
4.5 Nearest Two Neighbors	24

Chapter 5	A ring of non-identical oscillators	34
Chapter 6	Connecting two rings of oscillators	39
6.1	Coupling two rings of oscillators through one common node	40
6.2	Effects of coupling location on non-homogeneous rings	45
6.2.1	Case 1: Connecting oscillators from the fourth quadrant of ring X to the fourth quadrant of ring Y	46
6.2.2	Case 2: Connecting oscillators from the second quadrant of ring X to the second quadrant of ring Y	46
6.2.3	Case 3: Connecting oscillators from the second quadrant of ring X to the fourth quadrant of ring Y	48
6.2.4	Case 4: Connecting oscillators from the first quadrant of ring X to the first quadrant of ring Y	51
Chapter 7	Conclusion	54
	Bibliography	60
	Appendices	62
Appendix A	MATLAB code for figures	63

List of Figures

2.1	Visual representation of N_i in iteration $t+1$ as a function of N_{i-1} , N_i , and N_{i+1} in iteration t	6
2.2	Bifurcation plot of the Ricker Model given by Equation 2.2	7
4.1	Evolution of the second node with $m = 2$	14
4.2	Evolution of the first node with $m = 0$	15
4.3	Visualization of 4 period solution with $s = 1$	17
4.4	Solutions for each node with $s = 1$, $s = 14$, and $s = 16$	19
4.5	Response of all node values when $s = 1$	19
4.6	Evolution of the first node with $s = 29$	21
4.7	Response of all nodes when $s = 29$	21
4.8	Visualization of 4 period solution with $s = 29$	22
4.9	Largest 3 LCE values for $b = 0$ to 0.5 and $r = 3$	23
4.10	Periodicity of nodes 1 and 9 for $b = 0.25$	24
4.11	Largest 3 LCE values for $b = 0$ to 0.5 and $r = 4.6$	25
4.12	Visual representation of N_i in iteration $t + 1$ as a function of N_{i-2} , N_{i-1} , N_i , N_{i+1} and N_{i+2} in iteration t	26
4.13	Evolution of the first node with $m = 2$, $r = 4.6$, and $b = 0.2$	27
4.14	Evolution of the first node with $m = 4$, $r = 4.6$, and $b = 0.1$	31

5.1	A ring of non-homogeneous oscillators with $r = 3$ for the first 24 nodes and $r = 4.6$ for the last 8 nodes	35
5.2	Node locations from iteration 2,000,000 to iteration 2,002,000 based off of the four sets provided in Table 5.1	37
5.3	Largest 3 LCE values on a non-homogeneous ring for $b = 0$ to 0.5	38
6.1	Coupled rings	41
6.2	Evolution of the first node in ring X with $m = 2$ in coupled rings	42
6.3	All LCE values when $s = 1$ for ring X and $s = 2$ for ring Y	43
6.4	Largest three LCE values when $s = 1$ for ring X and $s = 2$ for ring Y for values of C from 0 to 1.5	44
6.5	(a) Visualization of coupling for case 1 with $r = 3$ for quadrants 1-3 and $r = 4.6$ for quadrant 4. (b) Numerical results for case 1.	47
6.6	(a) Visualization of coupling for case 2 with $r = 3$ for quadrants 1-3 and $r = 4.6$ for quadrant 4. (b) Numerical results for case 1.	49
6.7	(a) Visualization of coupling for case 3 with $r = 3$ for quadrants 1-3 and $r = 4.6$ for quadrant 4. (b) Numerical results for case 1.	50
6.8	(a) Visualization of coupling for case 4 with $r = 3$ for quadrants 1-3 and $r = 4.6$ for quadrant 4. (b) Numerical results for case 1.	52

List of Tables

4.1	Largest 5 LCEs for seed values $s = 1, 5, 10, 14, 16$ and 20	18
5.1	Largest 3 LCEs using four different sets of initial conditions on a non-homogeneous ring	36

Chapter 1

Introduction

One of the key factors in any population model is the intrinsic growth rate r . For many populations found in nature, regardless of the initial population, we expect to see the population stabilize over time. If the intrinsic growth rate increases, we would expect to see the equilibrium population increase and if the intrinsic growth rate decreases, we may see the equilibrium population decrease, and in some cases, the population might even go extinct. By plotting the equilibrium population against the intrinsic growth rate, we can come up with a bifurcation plot of the population model. As we observe the equilibrium population for given values of r , we may see the population bifurcate. That is, the equilibrium population can have multiple values. One year, the population might be higher while the next year it might be lower. After a second bifurcation, we may see four different equilibrium populations for a given value of r . As we continue to allow r to increase, we may observe more bifurcations in these population models. However, depending on the population model, we may reach values of r where the equilibrium population has no periodicity. Rather, for those values of r , the equilibrium population is chaotic.

As we continue to let r increase, we may find that the population that was once chaotic, may once again become periodic.

The Ricker model is one such model that has a bifurcation plot where we observe both periodic and chaotic equilibrium populations depending on the intrinsic growth rate. The Ricker model is a discrete population model that provides the density of a population N_{t+1} in generation $t + 1$ based on the density of the population N_t in generation t . This was introduced by Bill Ricker in 1954 to predict Fish stocks prices based on recruitment in fisheries and is the model of interest in this paper [3].

The usefulness of population models expands well beyond determining the population in a given generation. A period-doubling bifurcation to chaos was discovered in spontaneous firings of *Onchidium* pacemaker neurons [5]. In this study, scientists gave rabbits a drug that sent their hearts into fibrillation. On the path to fibrillation, they found a period doubling route to chaos. When the drug was administered, the heart was beating periodically. As time progressed, a period doubling occurred and causing a bifurcation on the regularity of the heart beat, meaning that the heart would beat in a two-cycle interval. As more time progressed, another period doubling occurred leading to the heart beating at a four-cycle interval. Until eventually, the heart would beat at a chaotic, unpredictable rate. The scientists successfully used chaos theory to monitor when to apply electrical shocks to the heart in order to return it to periodicity.

There are many more applications to these population models such as cryptography [6], robotics [7], and celestial mechanics [8]. An application that specifically uses the Ricker model stems from ecology in what is known as a scramble competition [9]. This is a competition in which a particular resource is available to all of

its competitors. However, because resources are mostly finite, the population of all competitors will decrease.

The synchronization behavior of coupled Ricker maps over a complex network is studied in [10]. While we will be focusing on a nearest neighbor approach for connecting oscillators, Poria, Khan, and Nag connect oscillators randomly, making their network more dynamic. In [11], Pade, Lucken, and Yanchuk study the destabilization mechanism in a unidirectional ring of identical oscillators, perturbed by the introduction of a long-range connection.

In this paper, we parallel the work done by Hubertus von Bremen in [1] by exploring rings of homogeneous and non-homogeneous oscillators. However, while von Bremen uses the function $f(x, \alpha) = 1 - \alpha x^2$ to explore these rings of coupled oscillators, we exclusively use the Ricker model given by $f(N, r) = N_t e^{r(1-N_t)}$. In both models, the oscillators or nodes can be reminiscent of neurons firing in the brain. We will explore rings of oscillators that, when acting independently, will exhibit a chaotic response. However, when these nodes are connected to their nearest neighbors, a periodic response emerges. In addition to connecting nodes to their nearest neighbors, we will connect nodes to their nearest two neighbors and observe the response. We will observe the effects that initial conditions have on these rings of oscillators, and we will see the system response when two rings are coupled together.

In chapter 2, we introduce the Ricker model and its bifurcation plot. In chapter 3, we explore Lyapunov Characteristic Exponents and how they can be used to determine the response of the system. In chapter 4, we explore a ring of identical oscillators. We will view the evolution of a single node, determine the effects initial conditions have on the system response, explore cases with symmetric node

responses, and determine the effects of changing the connection strength of the system. In chapter 5, we explore a ring of non-identical oscillators. And in the last chapter, we view the dynamical behavior emerging from coupling two rings of non-homogeneous oscillators.

Chapter 2

The Ricker Model

In this chapter we will introduce the Ricker model and its bifurcation plot. We observe regions of the bifurcation plot for which we obtain periodic solutions and regions for which we obtain a chaotic solution based on the intrinsic growth rate. Using this model, we can develop a ring of oscillators with each oscillator connected to its nearest neighbor. We hope to show that when oscillators are connected to their nearest neighbors, their solution becomes periodic, despite the chaotic nature of the individual oscillators.

We begin by connecting a single ring of n oscillators where the i th oscillator is given by the iterative equation

$$N_i(t+1) = bf(N_{i-1}(t), r_{i-1}) + af(N_i(t), r_i) + bf(N_{i+1}(t), r_{i+1}) \quad (2.1)$$

where $f(N, r)$ is the Ricker Model given by

$$f(N, r) = N_t e^{r(1-N_t)}. \quad (2.2)$$

Here the i th oscillator in the $t+1$ st iteration is a function of the i th oscillator and its two neighbors in the previous iteration. See Figure 2.1 for a visual representation.

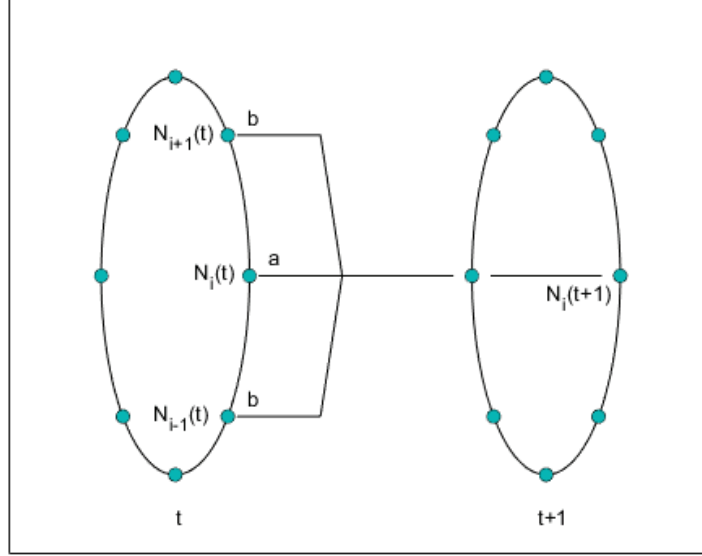


Figure 2.1: Visual representation of N_i in iteration $t + 1$ as a function of N_{i-1} , N_i , and N_{i+1} in iteration t

Since we are creating a ring of oscillators, we allow the 1st oscillator in the $t + 1$ st iteration to be a function of the n th, 1st, and 2nd oscillators in the previous iteration where n is the number of oscillators in the ring. Likewise, the n th oscillator in the $t + 1$ st iteration is a function of the $n - 1$ st, n th, and 1st oscillators of the previous iteration. a is the connection strength between iterations of the i th oscillator while b is the connection strength to each neighbor between iterations. In this paper, we let $a + mb = 1$ where m is the number of neighbors used to calculate $N_i(t + 1)$.

The bifurcation plot of the Ricker Model given by Equation 2.2 can be seen in Figure 2.2. We observe that for $1 \leq r < 2$ there is a periodicity of 1. For $2 \leq r < 2.53$, there is periodicity is 2. For $2.53 \leq r < 2.66$, there is a periodicity of 4. There are values of r , such as $r = 3$, where it appears that there may be chaotic

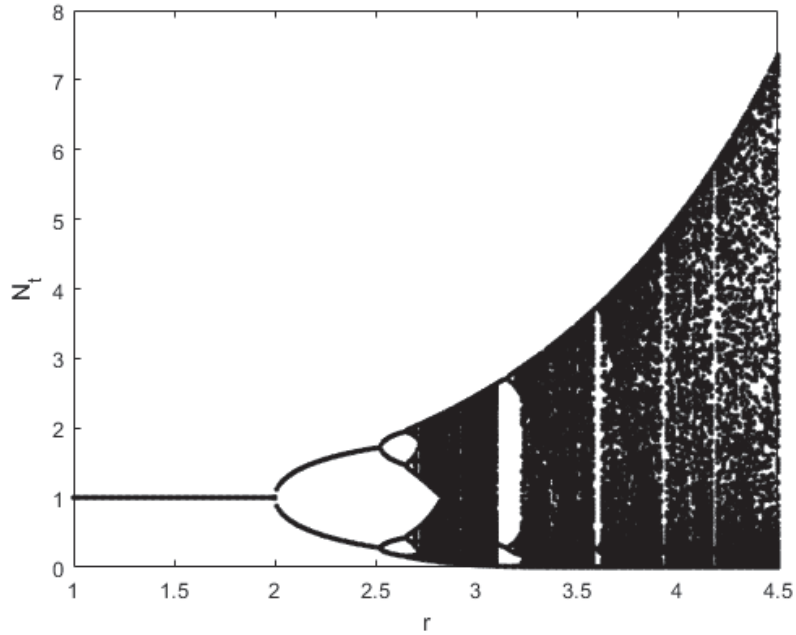


Figure 2.2: Bifurcation plot of the Ricker Model given by Equation 2.2

solutions.

In this chapter, we introduced the Ricker model and its bifurcation plot. We showed how this model can be used in a ring of oscillators with each oscillator connected to its nearest neighbors. In the bifurcation plot produced, we observed regions for which we observed periodic solutions and regions where the solutions were chaotic. It should be noted that depending on the intrinsic growth rate, the solution can go from periodic to chaotic and back to periodic. In the next chapter, we will discuss how to determine if a solution is periodic or chaotic.

Chapter 3

Lyapunov Characteristic Exponents

Lyapunov Characteristic Exponents (LCEs) are asymptotic measures characterizing the average rate of growth (or shrinking) of small perturbations to the solution of a dynamical system [4]. We can use LCEs to measure the divergence from perturbed initial conditions. In this paper, we will use LCEs to determine if a solution is chaotic or periodic with positive LCEs being chaotic.

Hubertus von Bremen provides a method called the Householder QR based method (HQRB) for the computation of LCEs in [2]. The following MATLAB code was created from the algorithm provided in [2]:

Listing 3.1: Calculating LCEs

```

1 function [ LCEvector ] = LCE( map, tanmap, iteration, lce_iteration, b, r, n, s )
2 LCEvector=zeros(n,1); % Initializing Variables
3 R=zeros(n,1);
4 [ N ] = feval( map, iteration+1, b, r, n, s ); % Create the map of N
5 Ni_1=N(iteration-lce_iteration+1,:); % Create 1st and 2nd tanmaps
6 Ni_2=N(iteration-lce_iteration+2,:);
7 [ tanmap1 ] = feval( tanmap, Ni_1, b, r, n );
8 [ tanmap2 ] = feval( tanmap, Ni_2, b, r, n );
9 for i=1:lce_iteration % QR-factorization
10     for k=1:n-1
11         sigma=sqrt(sum(tanmap1(k:n,k).^2)); % Computation of the reflectors
12         gamma=sigma*(sigma+abs(tanmap1(k,k)));
13         if tanmap1(k, k)<0
14             R(k)=sigma;
15         else
16             R(k)=-sigma;
17         end
18         tanmap1(k,k)=tanmap1(k,k)-R(k);
19         for j=k+1:n
20             beta=(tanmap1(k:n,k)'*tanmap1(k:n,j))/gamma;
21             tanmap1(k+1:n,j)=tanmap1(k+1:n,j)-tanmap1(k+1:n,k)*beta;
22         end
23         for j=1:n % Computation of action of tanmap2
24             beta=tanmap2(j,k:n)*tanmap1(k:n,k)/gamma;
25             tanmap2(j,k:n)=tanmap2(j,k:n)-tanmap1(k:n,k)'*beta;
26         end
27     end
28     R(n)=tanmap1(n,n);
29     if i=lce_iteration % Changing tanmap to next iteration
30         tanmap1=tanmap2; % New tanmap1
31         Ni_2=N(iteration-lce_iteration+2+i,:); % New tanmap2
32         [ tanmap2 ] = feval( tanmap, Ni_2, b, r, n );
33     end
34     LCEvector=LCEvector+log(abs(R));
35 end
36 LCEvector=LCEvector/lce_iteration;

```

In Listing 3.1, the inputs to the function, LCE , are map , $tanmap$, $iteration$, $lce_iteration$, b , r , n , and s . map is given by the iterative equation used to define the model such as in Equation 2.1. The $tanmap$ is given by the Jacobian of the map . $iteration$ is the total number of iterations. $lce_iteration$ is the total number of iterations used to calculate the LCE. b is the connection strength to each neighbor. r is the intrinsic growth rate seen in Equation 2.2. n is the total number of oscillators in the system and s is the seed number used for establishing initial conditions.

In this chapter, we introduced Lyapunov Characteristic Exponents and how they can be used to determine if a solution is periodic or chaotic. Positive LCEs indicate that a solution is chaotic while negative LCEs indicate that a solution is periodic. In order to use the HQRB method to calculate the LCEs, we need to construct a map and tangent map of the model. We will be developing a map and tangent map in the next chapter so that we can calculate the LCEs for the model we produced.

Chapter 4

A ring of identical oscillators

In section one, we begin our analysis by observing the evolution of a single node in a ring with 32 oscillators, each oscillator connected to its nearest neighbor. We will compare our results with a ring of 32 disconnected oscillators. We show how we develop initial conditions in this paper using seed values and we create a map tangent map of our connected ring.

In section two, we will explore the effects of changing the initial conditions by changing the seed value. We use the same ring with 32 oscillators with each oscillator connected to its nearest neighbor. Using six different seed values, we will calculate the 5 largest LCEs produced by the system and compare our results. We show an alternative method of comparing solutions of a system with the same periodicity by plotting the solutions against each other.

In section three, we observe a system with symmetric node responses. We investigate by plotting the evolution of a single node and by plotting the response of all nodes. We also provide a visualization of a four period solution.

In section four, we observe the effects of changing the connection strength, b ,

in a ring with 32 connected nodes, each node connected to its nearest neighbor when $r = 3$. We test the response of the connected ring by varying b from 0 to 0.5 and observe which values of the connection strength produce negative LCE values indicating a period solution. We then set $r = 4.6$ and again test the response of the connected ring by varying b from 0 to 0.5. Once we have the solutions to both systems for varying values of b , we compare our results.

In section five, we create a ring with 32 nodes, each node connected to its nearest two neighbors. We observe the evolution of a single node when $r = 4.6$. We compare our results to the results obtained from a connected ring with $r = 4.6$ but only connected to its nearest neighbors. We wish to see if a system that is more connected will yield more periodic solutions.

4.1 Evolution of a single node

In this section, we explore the evolution of a single node as we let our system evolve as in Equation 2.1. This means that we will have a coupled system with each node connected to its nearest neighbor ($m = 2$) through connection strength $b = 0.2$. Since we are letting $a + mb = 1$, $a = 0.6$. Here, we will be examining a $n = 32$ node system with intrinsic growth rate $r = 3$.

In this paper, initial conditions will be given by the MATLAB code `rand(seed , s)` and $N_0 = rand(1, n) + 0.5$ where s is the seed number and n is the number of oscillators in the system. This code will generate uniformly distributed random numbers between 0.5 and 1.5.

To generate the plot of an evolution of a single node, we must first establish a map of the Ricker Model with each node connected to its nearest neighbors. The

following MATLAB code will provide a map of the Ricker Model given by Equation 2.1:

Listing 4.1: Map of the Ricker Model with each node connected to its nearest neighbor

```

1 function [ N ] = map_ricker_nearestNeighbor ( iteration, b, r, n, s )
2 N=zeros(iteration, n); % Initial conditions
3 rand('seed', s)
4 N(1,:) = rand(1,n)+.5;
5 a=1-2*b;
6 for i=2:iteration      % Map of Ricker connecting to nearest neighbor
7     for j=1:n
8         if j==1
9             N(i,1)=b*(N(i-1,n)*exp(r*(1-N(i-1,n))))...
10                +a*(N(i-1,1)*exp(r*(1-N(i-1,1))))...
11                +b*(N(i-1,2)*exp(r*(1-N(i-1,2)))));
12         elseif j==n
13             N(i,n)=b*(N(i-1,n-1)*exp(r*(1-N(i-1,n-1))))...
14                +a*(N(i-1,n)*exp(r*(1-N(i-1,n))))...
15                +b*(N(i-1,1)*exp(r*(1-N(i-1,1)))));
16         else
17             N(i,j)=b*(N(i-1,j-1)*exp(r*(1-N(i-1,j-1))))...
18                +a*(N(i-1,j)*exp(r*(1-N(i-1,j))))...
19                +b*(N(i-1,j+1)*exp(r*(1-N(i-1,j+1)))));
20         end
21     end
22 end

```

Using the above parameters as inputs to Listing 4.1, we plot Figure 4.1. We can see that the node spontaneously changes from having chaotic response to what appears to be periodic. Initially, it may appear that the periodicity may be 2 between iterations 400 and 750, but there are minute oscillations in the mode response making the periodicity 4 in that interval. The periodicity of 4 becomes evident after 800 iterations.

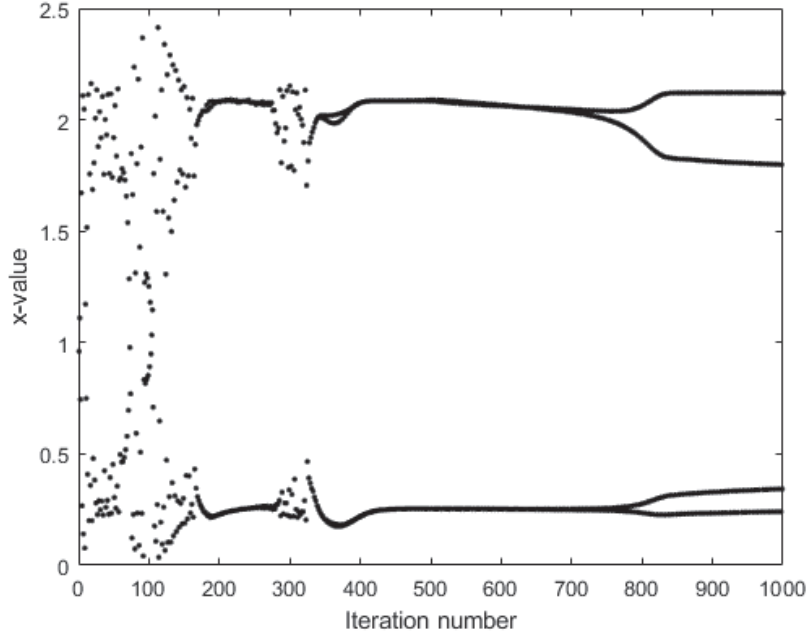


Figure 4.1: Evolution of the second node with $m = 2$

We can compare the evolution of the first node in a connected ring with the evolution of the first node in a disconnected ring given by Equation 2.2 using the same parameters above, but this time $b = 0$. Results for this case can be seen in Figure 4.2. This time, we do not see a change from a chaotic to periodic response of the first node in the first 800 iterations. In fact, even when $iteration = 2,000,000$, the node response remains chaotic.

We can verify if a solution is chaotic by determining the LCE for the system, with a positive LCE indicating a chaotic response. In order to do this, we use the same inputs used to create Figure 4.1 and Figure 4.2 in addition to the tangent map as seen in Listing 4.2. To compute the LCE for both cases, we let the system evolve for 2,000,000 iterations and take the next 50,000 iterations to calculate the LCE. Thus $iteration = 2,500,000$ and $lce_iteration = 50,000$. Using Listing 3.1,

we find that the LCE when $m = 2$ is -0.006 and 0.468 when $m = 0$. The results are as expected since we observed the first node to be periodic when $m = 2$ and chaotic when $m = 0$.

Listing 4.2: Tangent map of the Ricker Model with each node connected to its nearest neighbor

```

1 function [ tanmap ] = tanmap_ricker_nearestNeighbor ( Ni, b, r, n )
2 a=1-2*b;           % Initial conditions
3 tanmap=zeros(n);
4 for i=1:n          % Tangent map
5     if i==1
6         tanmap(1,n)=b*(exp(r*(1-Ni(n)))*(1-r*Ni(n)));
7         tanmap(1,1)=a*(exp(r*(1-Ni(1)))*(1-r*Ni(1)));
8         tanmap(1,2)=b*(exp(r*(1-Ni(2)))*(1-r*Ni(2)));
9     elseif i==n
10        tanmap(n,n-1)=b*(exp(r*(1-Ni(n-1)))*(1-r*Ni(n-1)));
11        tanmap(n,n)=a*(exp(r*(1-Ni(n)))*(1-r*Ni(n)));
12        tanmap(n,1)=b*(exp(r*(1-Ni(1)))*(1-r*Ni(1)));
13    else
14        tanmap(i,i-1)=b*(exp(r*(1-Ni(i-1)))*(1-r*Ni(i-1)));
15        tanmap(i,i)=a*(exp(r*(1-Ni(i)))*(1-r*Ni(i)));
16        tanmap(i,i+1)=b*(exp(r*(1-Ni(i+1)))*(1-r*Ni(i+1)));
17    end
18 end

```

To further demonstrate the periodic nature of the node response in a coupled system with $r = 3$, a visualization of the 4 period solution is seen in Figure 4.3. The circles represent the node number in the 32 node system while the diamonds represent the value of each node. The 8th and 24th node are given by the filled circles and the 7th, 8th, and 9th nodes are labeled as such. The four subplots shown represent the response of the 32 node system from iteration 2,000,000 to iteration 2,000,003. We can see that in each iteration plotted, the node responses are oscillating and that the cycle is complete between the 32nd node and 1st node.

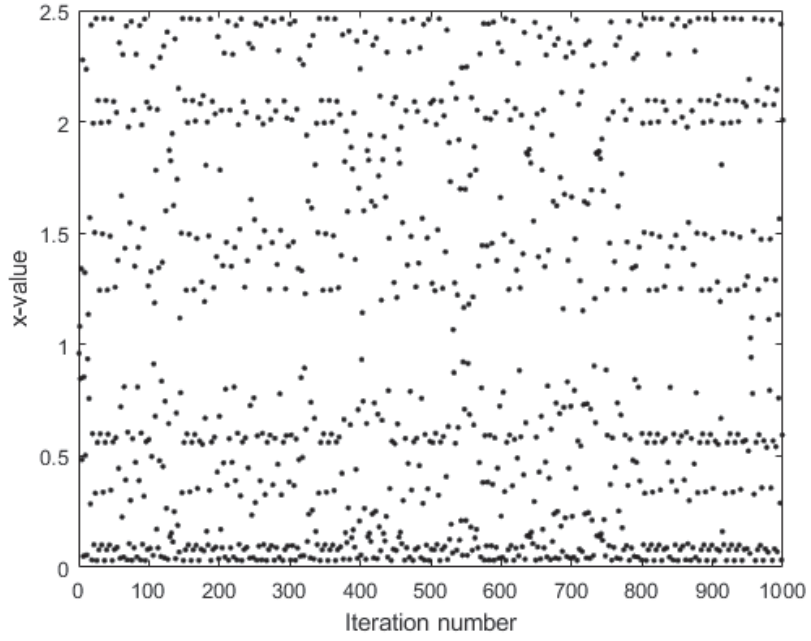


Figure 4.2: Evolution of the first node with $m = 0$

We can also see that each node takes on a new value with each iteration. Since this is a system with periodicity four, after 2,000,000 iterations, each node will cycle through each of the four values of $N_i(t)$.

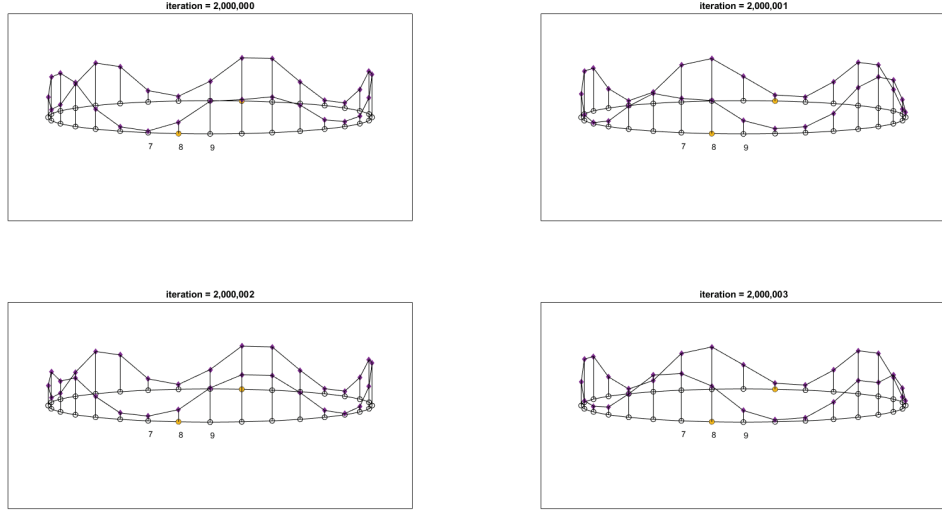


Figure 4.3: Visualization of 4 period solution with $s = 1$

4.2 Effect of changing the seed value

In the previous section, we explored the evolution of a single node with a seed $s = 1$. In this section we will observe the effect of changing the seed value as one of the initial conditions. We will use the same initial conditions provided in the last section; that is $iteration = 2,050,000$, $lce_iteration = 50,000$, $b = 0.2$, $r = 3$, $n = 32$, map provided by Listing 4.1, and $tanmap$ provided by Listing 4.2. Again, this means that we will let the system evolve for 2,000,000 iterations and use the next 50,000 iterations to calculate the LCEs. We will observe seed values $s = 1, 5, 10, 14, 16$ and 20 .

From Table 4.1, we see that changing the seed value as one of the initial conditions changes LCE values. However, in this case, we see that despite changing the seed values, the largest 5 LCE values remain negative for every seed chosen meaning that the solution is periodic. Investigating further, we find that the periodicity is

4 for all six seed values.

Table 4.1: Largest 5 LCEs for seed values $s = 1, 5, 10, 14, 16$ and 20

	$s = 1$	$s = 5$	$s = 10$	$s = 14$	$s = 16$	$s = 20$
LCEs	-0.0054	-0.0070	-0.0106	-0.0063	-0.0192	-0.0148
	-0.0083	-0.0332	-0.0353	-0.0198	-0.0222	-0.0149
	-0.0237	-0.0332	-0.0353	-0.0198	-0.0246	-0.0377
	-0.0359	-0.0448	-0.0419	-0.0343	-0.0319	-0.0392
	-0.0371	-0.0551	-0.0551	-0.0481	-0.0420	-0.0551

We can directly compare node values obtained using various initial conditions by plotting the node values together after the system has stabilized. However, this may be difficult to do if we are to compare a particular solution with every rotation of another solution. To simplify this process, we arrange the node values in a solution from least to greatest which allows us to easily compare our results. To ensure that the system has stabilized, we allow it to evolve for 2,000,000 iterations. We will use the same values of b , r , and n as we did above. We will compare solutions generated using seed values $s = 1, 14$ and 16 .

Figure 4.4 shows all possible solutions for $s = 1$, $s = 14$, and $s = 16$. Since there are 32 nodes and each solution has periodicity 4, there are $32 \times 4 = 128$ possible solutions for each seed value. In the next section, we will explore cases where the node values are symmetric and we will only obtain a total of 64 possible solutions. The blue squares represent node values when $s = 1$, the red diamonds represent node values when $s = 14$, and the yellow circles represent node values when $s = 16$. We can see that when we change our initial conditions by changing the seed, the

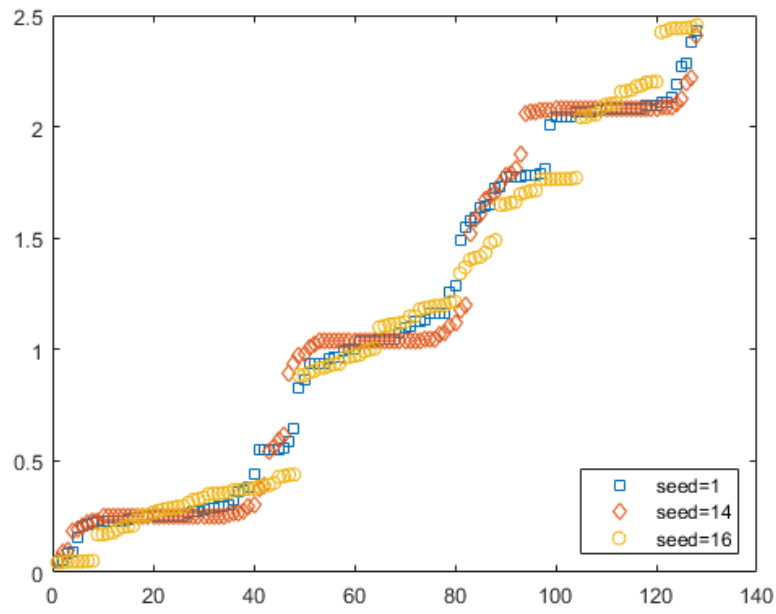


Figure 4.4: Solutions for each node with $s = 1$, $s = 14$, and $s = 16$

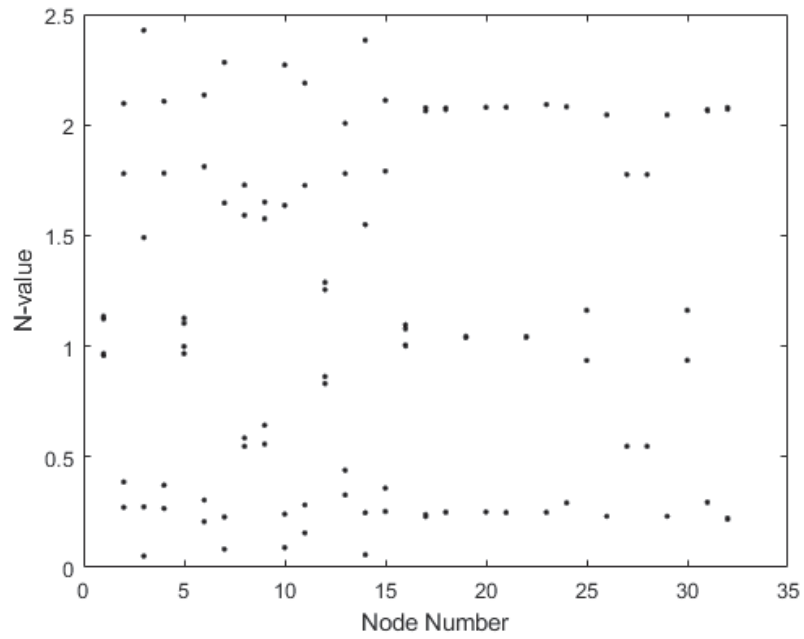


Figure 4.5: Response of all node values when $s = 1$

response to the system also changes. In Figure 4.5, we can see all 128 possible node values for each node in the system. Notice how each node has 4 values and how no two nodes share a response, confirming that there are 128 possible solutions.

4.3 Symmetric node responses

In this section, we will explore a system with symmetric node responses. Initial conditions are given by $iteration = 2,000,000$, $b = 0.2$, $r = 3$, $n = 32$ and $m = 2$. Using Listing 4.1, we plot the evolution of the first node with $s = 29$. In Figure 4.6, it appears that the system settles into a 2 period solution, but it is actually a 4 period solution. Because this is a symmetric solution, there are a total of $32 \times 2 = 64$ possible solutions. We can see this by plotting the response of each node seen in Figure 4.7. Notice the clear symmetry about the 16th Node Number.

The symmetry can also be seen by plotting the periodic solution in a ring as we did in Figure 4.3. Again, the circles represent each node, the diamonds represent the node responses, the filled circles represent the 8th and 24th nodes, and nodes 7, 8 and 9 are labeled as such. The four subplots shown represent the response of the 32 node system from iteration 2,000,000 to iteration 2,000,003. We can see that in Figure 4.8, the 8th and 9th nodes have the same node responses for each iteration plotted. Testing all possible seed values for the initial conditions given above, we find that all possible solutions have either 64 or 128 possible solutions.

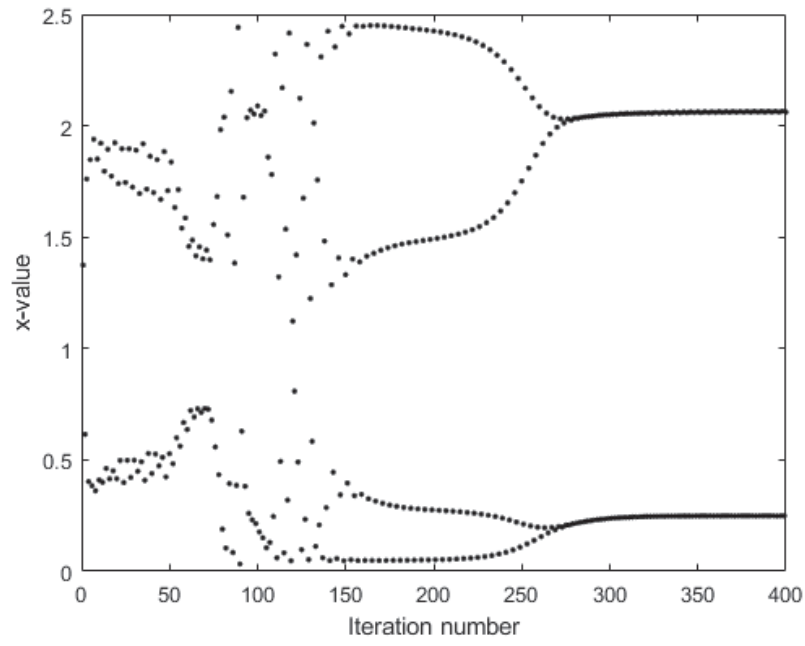


Figure 4.6: Evolution of the first node with $s = 29$

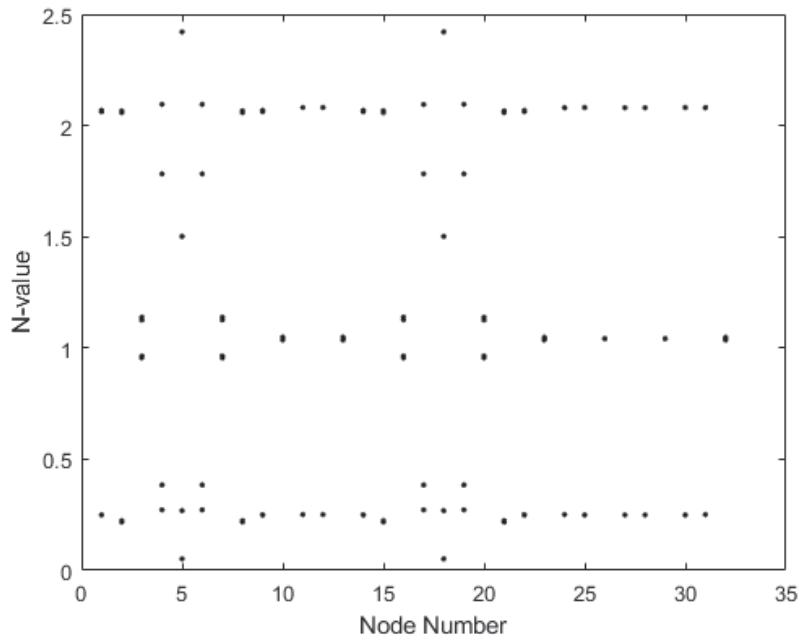


Figure 4.7: Response of all nodes when $s = 29$

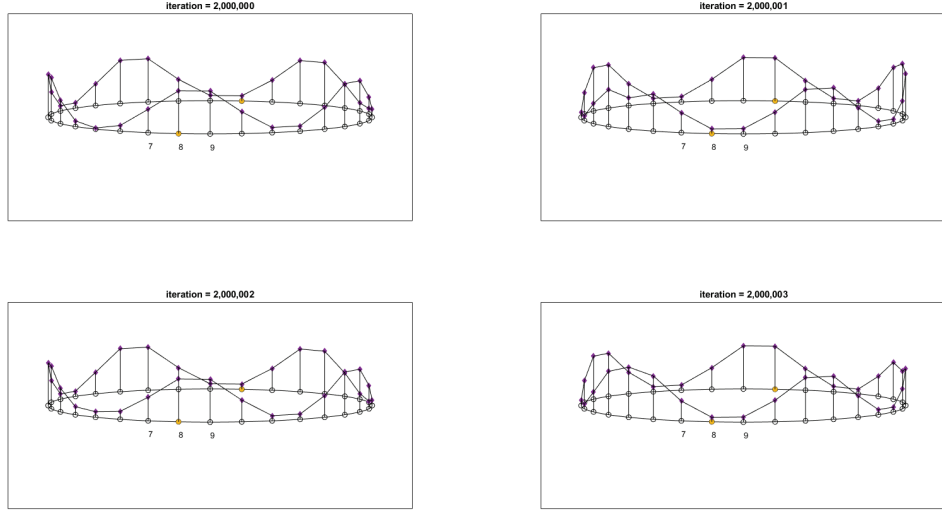


Figure 4.8: Visualization of 4 period solution with $s = 29$

4.4 Effect of changing the connection strength

We have already explored the difference between an uncoupled system and a system where $b = 0.2$. Now, we will explore values of b from 0 to 0.5. We do this by determining the largest 3 LCE values for each value of b . Recall that positive LCE values are indicative of chaotic solutions. Also recall that a can be determined by the equation $a + 2b = 1$ when $m = 2$. We will allow the system to evolve for 2,000,000 iterations and take the next 50,000 iterations to calculate the LCEs. Initial conditions are given by $iteration = 2,050,000$, $lce_iteration = 50,000$, $r = 3$, $n = 32$ and $s = 1$. map and $tanmap$ are given by Listings 4.1 and 4.2, respectively. Figure 4.9 displays the largest 3 LCE values for values of b from 0 to 0.5.

We can see from Figure 4.9 that most values of b yield LCE values less than 0 indicating a periodic solution. Specifically, observe that when $b = 0.02$, the LCE

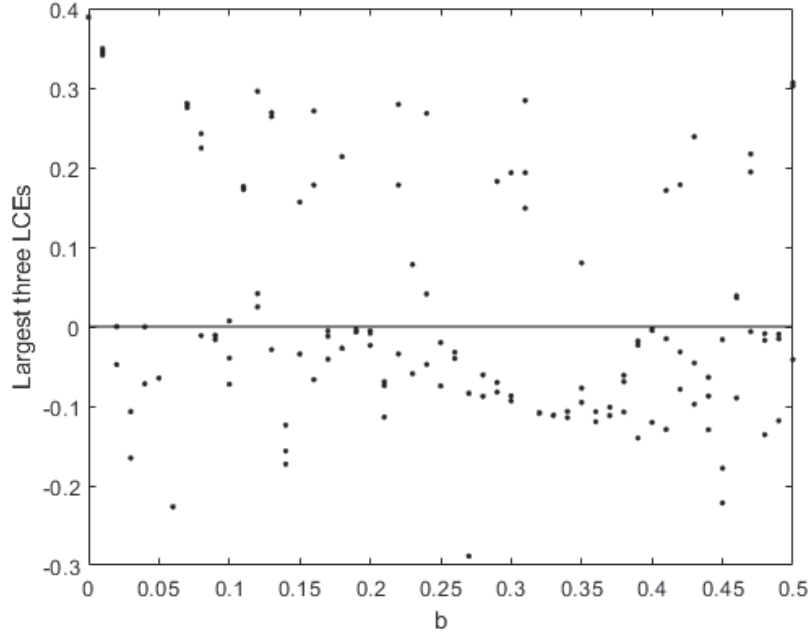


Figure 4.9: Largest 3 LCE values for $b = 0$ to 0.5 and $r = 3$

values are negative. This result was observed in Figure 4.1 where the solution became periodic between iteration 300 and 400. Also note that when $b = 0$ (an uncoupled system), we had a chaotic response which was observed in Figure 4.2. There seems to be no specific pattern as to which values of b provide negative LCEs.

To further explore the LCE values provided in Figure 4.9, we can observe the behavior of the system for $b = 0.25$ after 2,000,000 iterations. We can see that when $b = 0.25$, the largest three LCEs are negative. Each node in the system can have different periodicity, and in this example we observe a periodicity of 8 from the first node and a periodicity of 4 from the 9th node.

We have just demonstrated how changing the connection strength can affect the periodicity of the solution when $r = 3$. We will now change the connection strength of the system when $r = 4.6$. Just as we did above, we allow the system to evolve

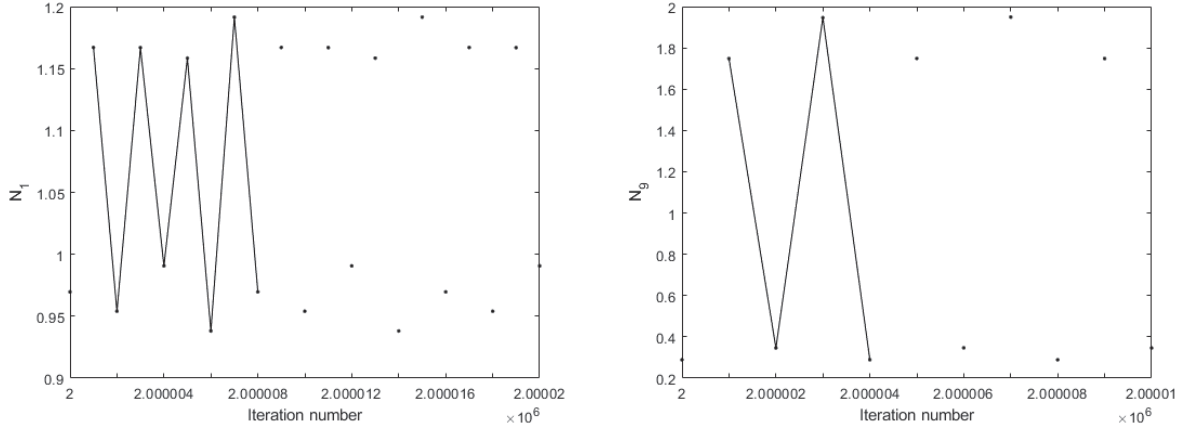


Figure 4.10: Periodicity of nodes 1 and 9 for $b = 0.25$

for 2,000,000 iterations and take the next 50,000 iterations to calculate the LCEs.

We will use the initial conditions from above, except this time $r = 4.6$.

For this value of r we can see that for a strongly connected system ($b = 0.08$ to 0.44), we have positive LCEs indicating a chaotic response. Only at the endpoints ($b < 0.08$ and $b > 0.44$) do we see negative LCEs. However, it should be noted that at $b = 0$, we have positive LCEs meaning that a disconnected system would not yield a periodic response.

4.5 Nearest Two Neighbors

So far, we have connected the nearest neighbor on each side of the oscillator. In this section, we will connect the nearest two neighbors on each side of the oscillators.

Expanding on equation 2.1, we obtain the following iterative equation:

$$\begin{aligned}
 N_i(t+1) = & bf(N_{i-2}(t), r_{i-2}) + bf(N_{i-1}(t), r_{i-1}) + af(N_i(t), r_i) + \\
 & bf(N_{i+1}(t), r_{i+1}) + bf(N_{i+2}(t), r_{i+2})
 \end{aligned} \tag{4.1}$$

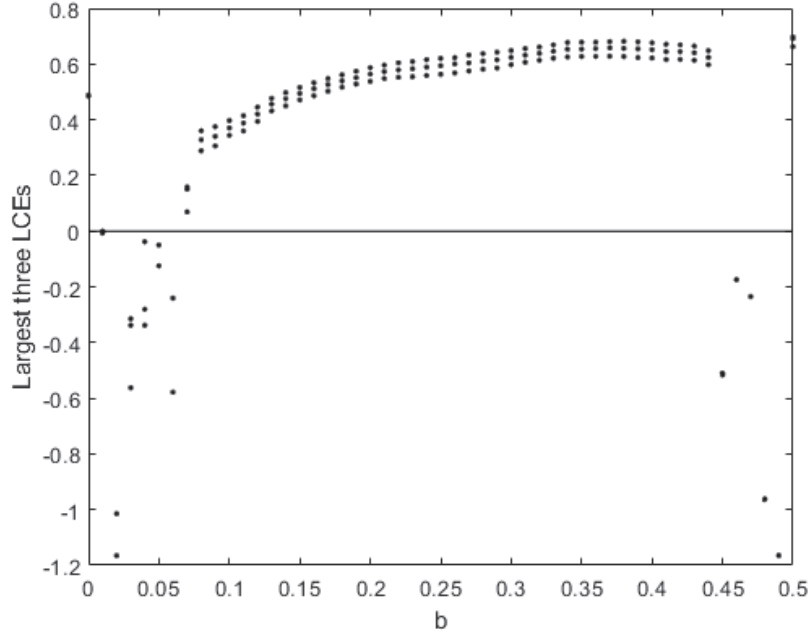


Figure 4.11: Largest 3 LCE values for $b = 0$ to 0.5 and $r = 4.6$

where $f(N, r) = N_t e^{r(1-N_t)}$. Here the i th oscillator in the $t + 1$ st iteration is a function of the i th oscillator and its four neighbors in the previous generation. Since we are creating a ring of oscillators, we allow the 1st oscillator in the $t + 1$ st iteration to be a function of the $n - 1$ st, n th, 1st, 2nd, and 3rd oscillators in the previous generation where n is the number of oscillators in the ring. Likewise, the n th oscillator in the $t + 1$ st iteration is a function of the $n - 2$ nd, $n - 1$ st, n th, 1st, and 2nd oscillators of the previous iteration. Additionally, since we are connecting the two nearest neighbors on each side of the oscillator, we must also account for the i th oscillator when $i = n - 1$ and when $i = 2$. When $i = n - 1$, it is a function of the $n - 3$ rd, $n - 2$ nd, $n - 1$ st, n th, and 1st oscillator of generation t . When $i = 2$, it is a function of the n th, 1st, 2nd, 3rd and 4th oscillators in generation t . See Figure 4.12 for a visualization. a is the connection strength between iterations of

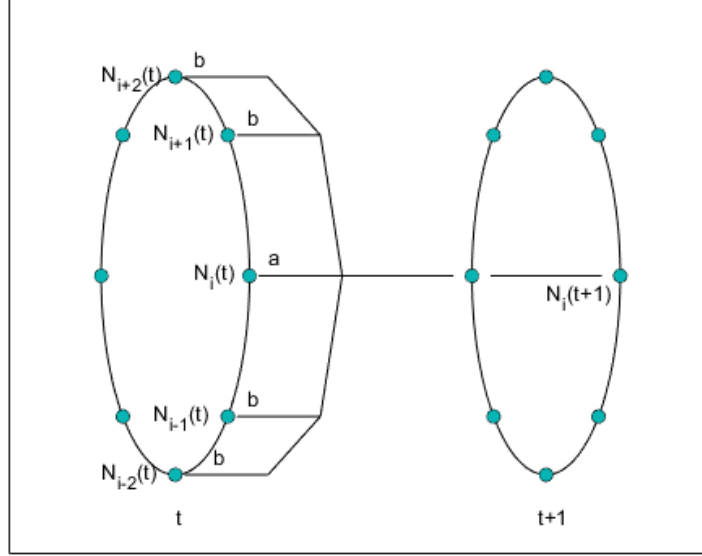


Figure 4.12: Visual representation of N_i in iteration $t + 1$ as a function of N_{i-2} , N_{i-1} , N_i , N_{i+1} and N_{i+2} in iteration t

the i th oscillator while b is the connection strength to each neighbor. Again, we let $a + mb = 1$.

In this section we wish to see if a system with each oscillator connected to its four nearest neighbors, two on each side, will lead to fewer chaotic solutions than when connected to just one neighbor on each side of the oscillator. As an example, we will examine the results for $r = 4.6$. From Figure 4.11, we saw LCEs less than 0 for $b < 0.07$ and $b > 0.44$. When $0.06 < b < 0.45$ we saw positive LCE values. One such value was $b = 0.2$. First we will examine the evolution of the first node when each oscillator is connected to its nearest neighbor ($m = 2$). We should expect to see a chaotic response. We will let the system evolve for 2,000,000 iterations. For this plot, $b = 0.2$, $r = 4.6$, $n = 32$ and $s = 1$.

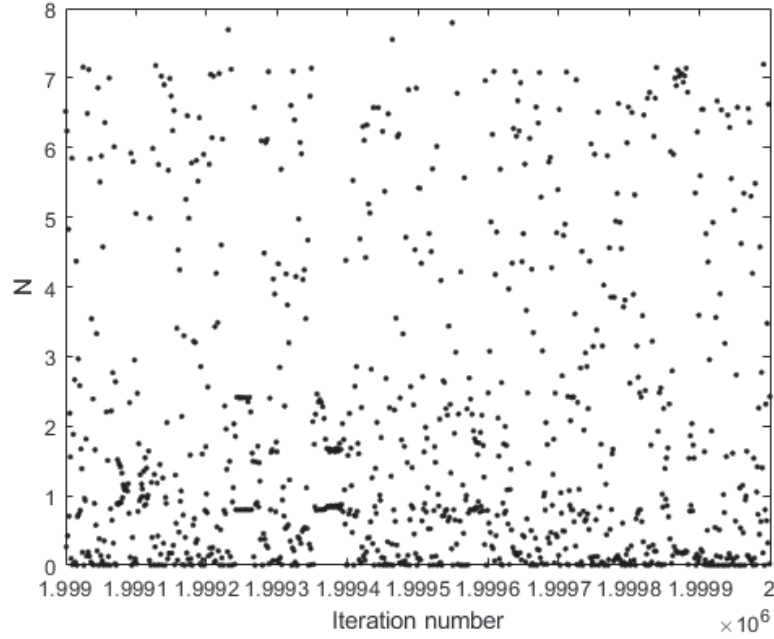


Figure 4.13: Evolution of the first node with $m = 2$, $r = 4.6$, and $b = 0.2$

We can see from Figure 4.13 a chaotic node response, even up to 2,000,000 iterations. This result was expected from our findings in Figure 4.11.

To determine if the system is still chaotic when $m = 4$, we must establish a map and tangent map to use for our LCE calculations. The map of the Ricker model when $m = 4$ can be created using Equation 4.1 and we can determine the tangent map by taking the Jacobian of the map. Both the map and tangent map can be seen in Listing 4.3 and 4.4.

Listing 4.3: Map of the Ricker Model with Oscillators Connected to their Nearest 4 Neighbors

```

1 function [ N ] = map_ricker_nearest4Neighbors ( iteration, b, r, n, s )
2 %Initial conditions
3 N=zeros(iteration, n);
4 rand('seed', s)
5 N(1,:) = rand(1,n)+.5;
6 a=1-4*b;
7 %Map of Ricker connecting to nearest 4 neighbors
8 for i=2:iteration
9     for j=1:n
10         if j==2
11             N(i,2)=b*(N(i-1,n)*exp(r*(1-N(i-1,n))))...
12                 +b*(N(i-1,1)*exp(r*(1-N(i-1,1))))...
13                 +a*(N(i-1,2)*exp(r*(1-N(i-1,2))))...
14                 +b*(N(i-1,3)*exp(r*(1-N(i-1,3))))...
15                 +b*(N(i-1,4)*exp(r*(1-N(i-1,4))));
16         elseif j==1
17             N(i,1)=b*(N(i-1,n-1)*exp(r*(1-N(i-1,n-1))))...
18                 +b*(N(i-1,n)*exp(r*(1-N(i-1,n))))...
19                 +a*(N(i-1,1)*exp(r*(1-N(i-1,1))))...
20                 +b*(N(i-1,2)*exp(r*(1-N(i-1,2))))...
21                 +b*(N(i-1,3)*exp(r*(1-N(i-1,3))));
22         elseif j==n
23             N(i,n)=b*(N(i-1,n-2)*exp(r*(1-N(i-1,n-2))))...
24                 +b*(N(i-1,n-1)*exp(r*(1-N(i-1,n-1))))...
25                 +a*(N(i-1,n)*exp(r*(1-N(i-1,n))))...
26                 +b*(N(i-1,1)*exp(r*(1-N(i-1,1))))...
27                 +b*(N(i-1,2)*exp(r*(1-N(i-1,2))));
28         elseif j==n-1
29             N(i,n-1)=b*(N(i-1,n-3)*exp(r*(1-N(i-1,n-3))))...
30                 +b*(N(i-1,n-2)*exp(r*(1-N(i-1,n-2))))...
31                 +a*(N(i-1,n-1)*exp(r*(1-N(i-1,n-1))))...
32                 +b*(N(i-1,n)*exp(r*(1-N(i-1,n))))...
33                 +b*(N(i-1,1)*exp(r*(1-N(i-1,1))));
34         else
35             N(i,j)=b*(N(i-1,j-2)*exp(r*(1-N(i-1,j-2))))...

```

```

36         +b*(N(i-1,j-1)*exp(r*(1-N(i-1,j-1))))...
37         +a*(N(i-1,j)*exp(r*(1-N(i-1,j))))...
38         +b*(N(i-1,j+1)*exp(r*(1-N(i-1,j+1))))...
39         +b*(N(i-1,j+2)*exp(r*(1-N(i-1,j+2)))));
40     end
41 end
42 end

```

Listing 4.4: Tangent Map of the Ricker Model with Oscillator Connected to their Nearest 4 Neighbors

```

1 function [ tanmap ] = tanmap_ricker_nearest4Neighbors ( Ni, b, r, n )
2 %Initial conditions
3 a=1-4*b;
4 tanmap=zeros(n);
5 %Find tangent map
6 for i=1:n
7     if i==2
8         tanmap(2,n)=b*(exp(r*(1-Ni(n)))*(1-r*Ni(n)));
9         tanmap(2,1)=b*(exp(r*(1-Ni(1)))*(1-r*Ni(1)));
10        tanmap(2,2)=a*(exp(r*(1-Ni(2)))*(1-r*Ni(2)));
11        tanmap(2,3)=b*(exp(r*(1-Ni(3)))*(1-r*Ni(3)));
12        tanmap(2,4)=b*(exp(r*(1-Ni(4)))*(1-r*Ni(4)));
13
14    elseif i==1
15        tanmap(1,n-1)=b*(exp(r*(1-Ni(n-1)))*(1-r*Ni(n-1)));
16        tanmap(1,n)=b*(exp(r*(1-Ni(n)))*(1-r*Ni(n)));
17        tanmap(1,1)=a*(exp(r*(1-Ni(1)))*(1-r*Ni(1)));
18        tanmap(1,2)=b*(exp(r*(1-Ni(2)))*(1-r*Ni(2)));
19        tanmap(1,3)=b*(exp(r*(1-Ni(3)))*(1-r*Ni(3)));
20
21    elseif i==n
22        tanmap(n,n-2)=b*(exp(r*(1-Ni(n-2)))*(1-r*Ni(n-2)));
23        tanmap(n,n-1)=b*(exp(r*(1-Ni(n-1)))*(1-r*Ni(n-1)));
24        tanmap(n,n)=a*(exp(r*(1-Ni(n)))*(1-r*Ni(n)));
25        tanmap(n,1)=b*(exp(r*(1-Ni(1)))*(1-r*Ni(1)));
26        tanmap(n,2)=b*(exp(r*(1-Ni(2)))*(1-r*Ni(2)));
27

```

```

28     elseif i==n-1
29         tanmap(n-1,n-3)=b*(exp(r*(1-Ni(n-3)))*(1-r*Ni(n-3)));
30         tanmap(n-1,n-2)=b*(exp(r*(1-Ni(n-2)))*(1-r*Ni(n-2)));
31         tanmap(n-1,n-1)=a*(exp(r*(1-Ni(n-1)))*(1-r*Ni(n-1)));
32         tanmap(n-1,n)=b*(exp(r*(1-Ni(n)))*(1-r*Ni(n)));
33         tanmap(n-1,1)=b*(exp(r*(1-Ni(1)))*(1-r*Ni(1)));
34
35     else
36         tanmap(i,i-2)=b*(exp(r*(1-Ni(i-2)))*(1-r*Ni(i-2)));
37         tanmap(i,i-1)=b*(exp(r*(1-Ni(i-1)))*(1-r*Ni(i-1)));
38         tanmap(i,i)=a*(exp(r*(1-Ni(i)))*(1-r*Ni(i)));
39         tanmap(i,i+1)=b*(exp(r*(1-Ni(i+1)))*(1-r*Ni(i+1)));
40         tanmap(i,i+2)=b*(exp(r*(1-Ni(i+2)))*(1-r*Ni(i+2)));
41     end
42 end

```

To compare our results of a system with two connected oscillators as seen in Figure 4.13, we will plot a system of 32 oscillators with each oscillator connected to their nearest four neighbors as seen in Figure 4.12. Figure 4.14 was created using Listing 4.3 with $iteration = 3000$, $b = 0.1$, $r = 4.6$, $n = 32$ and $s = 1$.

We can see from Figure 4.14 a change from a chaotic solution to what may be a periodic solution between iteration 1,000 and 1,500. After 1,500 iterations, it appears that the first node only attains 2 values and that the solution is not chaotic. To verify, we need to find the LCE's. By allowing the system to evolve for 2,000,000 iterations and using the next 50,000 iterations to calculate the LCE's, we obtain a max LCE value of -0.055 which verifies that the solution is periodic.

It is important to note that in making the comparison between a system with 2 connected neighbors ($m = 2$) and a system with 4 connected neighbors ($m = 4$), the value that is fixed is a , the connection strength from the same node between generations. Given that $a + mb = 1$ with $a = 0.6$, when $m = 2$, $b = 0.2$, and when $m = 4$, $b = 0.1$. We were able to see a case where a system with 4 connected neigh-

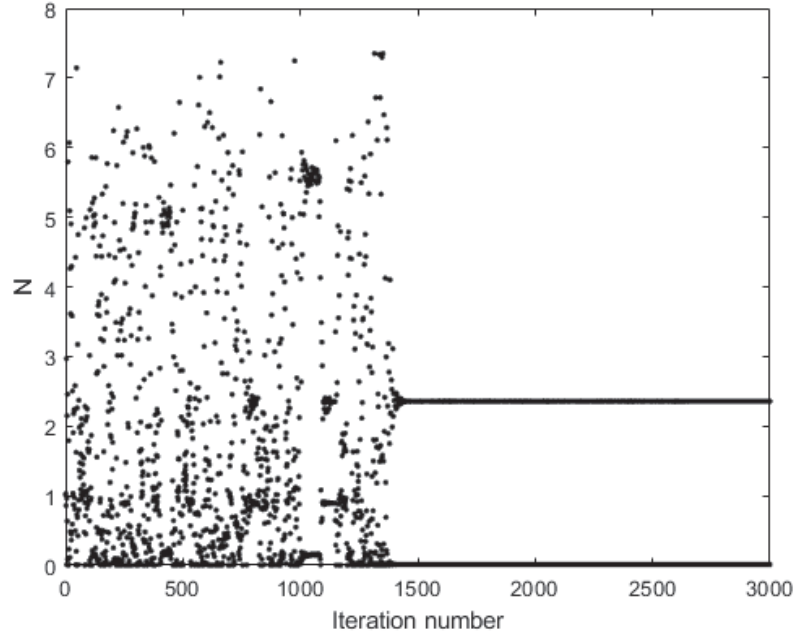


Figure 4.14: Evolution of the first node with $m = 4$, $r = 4.6$, and $b = 0.1$

bors yielded periodic results where as a system with only 2 connected neighbors did not.

In section one, we began our analysis by observing the evolution of a single node in a ring with 32 oscillators with each oscillator connected to its nearest neighbor. We found that the observed node exhibited a chaotic response that eventually turned periodic with a periodicity of four. However, when we conducted this analysis with the same initial conditions except without connecting the nearest neighbors, we found that the system remained chaotic, even after 2,000,000 iterations. In order to determine if the system was indeed chaotic, we developed a map and tangent map for use in calculating LCEs and found the the disconnected system was chaotic while the system with each node connected to its nearest neighbor was periodic.

In section two, explored the effects of changing the initial conditions by changing the seed values. We used a system where each node was connected to its nearest neighbor and calculated the largest 5 LCEs with initial conditions produced using six different seed values. For each seed chosen, we found that the LCE values were different, but in all six cases, the largest five LCEs remained negative and the system for each case had a periodicity of four. We could further explore these results to see if we can find a system that is periodic with certain seed values and chaotic with others. Because the system observed was periodic, with each node having periodicity four, there were $32 \times 4 = 128$ possible solutions for each seed value observed. We arranged the node responses from smallest to largest to make a comparison between the node responses of each system. We found that changing the initial conditions by using different seed values generate different solutions for each system.

In section three, we observed a system with a symmetric response. The system that we observed appeared to have a two period solution, but it was actually a four period solution that was symmetric. We were able to show the symmetry by plotting the periodic solution in a ring and observing which nodes had the same node response. We found that all of the seed values tested produced either 64 or 128 possible solutions depending on whether or not the system was symmetric.

In section four, we observed the effects of changing the connection strength, b , in a ring with 32 connected nodes, each node connected to its nearest neighbor. We had already explored the system response when the connection strength was $b = 0.2$. We then tested the response of the connected ring by varying b from 0 to 0.5 and observed the largest 3 LCEs produced for each value of b . We found that in a connected ring for the initial conditions used, specifically $r = 3$, that most of

the values of b produced a periodic response. We then set $r = 4.6$ and found the largest 3 LCEs for each value of b when b was varied from 0 and 0.5. With $r = 4.6$ in a system where each node is connected to its nearest neighbor, we found that most of the LCEs were positive indicating a chaotic response.

In section five, we created a ring with 32 nodes, each node connected to its nearest two neighbors. We observed the evolution of a single node with the intrinsic growth rate $r = 4.6$. This value of the intrinsic growth rate was used because we had previously found that for this node, given the initial conditions, in a system where only the nearest neighbors were connected, there was a chaotic response. By connecting more nodes in the system, we were able to turn a response that was previously chaotic into a periodic response. In this paper, we observed results of rings of oscillators in a disconnected system, a ring with nodes connected to their nearest neighbors, and a ring with nodes connected to their nearest two neighbors. It seems as though the more connected the system is, the more likely it is for the node responses to become periodic. Further analysis would include connecting more nodes, including a ring that is completely connected. Such a ring was not tested in this paper because it was too computationally expensive.

Chapter 5

A ring of non-identical oscillators

In the previous chapter, we explored a ring of identical oscillators with various initial conditions. We will now explore a ring of non-identical oscillators where the first 24 nodes have intrinsic growth rate $r = 3$ and the last 8 nodes have intrinsic growth rate $r = 4.6$. We will test this ring using four different sets of initial conditions and determine the LCE values given in each set. We will conduct further analysis by plotting the node locations of all 32 nodes for each set of initial conditions. We will also observe the response of the system when varying the connection strength b and determine if the solutions given are periodic or chaotic.

We begin by providing a visualization of the ring configuration used in this chapter. Figure 5.1 provides an illustration of this configuration. Note that this example was created using Equation 2.1 since we can see that each node is connected to its nearest neighbor. We can also see that a single node can be connected to a neighbor with $r = 3$ and another neighbor with $r = 4.6$.

To demonstrate the effects initial conditions have on a non-homogeneous ring we will let the system evolve using four different sets of initial conditions. The

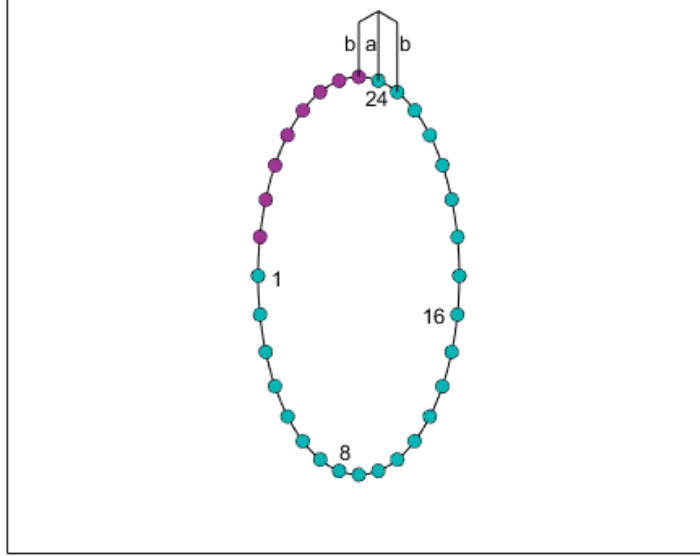


Figure 5.1: A ring of non-homogeneous oscillators with $r = 3$ for the first 24 nodes and $r = 4.6$ for the last 8 nodes

first two sets of initial conditions will be generated using the sinusoidal equation $N_j(0) = \mu \sin(v\pi(j-1)/(n-1)) + 1$. In set 1, we let $\mu = 0.1$ and $v = 5$. In set 2, we let $\mu = 0.85$ and $v = 5$. In set 3, initial conditions are randomly generated as before with seed $s = 1$. Finally, in set 4, initial conditions are randomly generated as before with seed $s = 10$.

To measure the effects of the initial conditions, the three largest LCEs are generated using initial conditions from each set and can be seen in Table 5.1. To generate the LCEs we use *map* and *tanmap* generated through a modification of Listing 4.1 and 4.2, respectively. Initial conditions were modified appropriately from above and the value of r is given by Figure 5.1. In each case, the system is allowed to evolve for 2,000,000 iterations and the next 50,000 iterations were used

to calculate the LCEs and we let the connection strength $b = 0.2$.

Table 5.1: Largest 3 LCEs using four different sets of initial conditions on a non-homogeneous ring

	Set 1	Set 2	Set 3	Set 4
LCEs	-0.0033	-0.0148	-0.0025	-0.0095
	-0.0262	-0.0268	-0.0268	-0.0377
	-0.0262	-0.0415	-0.0268	-0.0560

We can see from Table 5.1 that all four sets yield negative values for the three largest LCEs suggesting that the solution in all four sets are periodic. However, it is important to note that the largest 3 LCEs have values very close to 0 and require further investigation. Although the three largest LCEs are negative in each set, they are different from one another. To help identify the difference, we will plot the location of each node for each of the four cases which will help us see the attractors and we can determine if the solutions are indeed periodic.

In Figure 5.2, we record the location of each node from iteration 2,000,000 to iteration 2,002,000 for the four sets provided in Table 5.1. In the last three sets, we can see that most nodes are periodic but nodes 26 through 31 seem to be chaotic based on the figure. It may be the case that all nodes in the first set could be periodic with higher periodicity on nodes 26 through 31. In the last three sets, for nodes 25 and 32, it appears that most of the node locations reside between locations 4.7 and 6.5. Observing all four cases, we can see that locations are unique in each which suggests that the initial conditions affect the location of the attractors.

To show the system response of a non-homogeneous ring with the first 24 os-

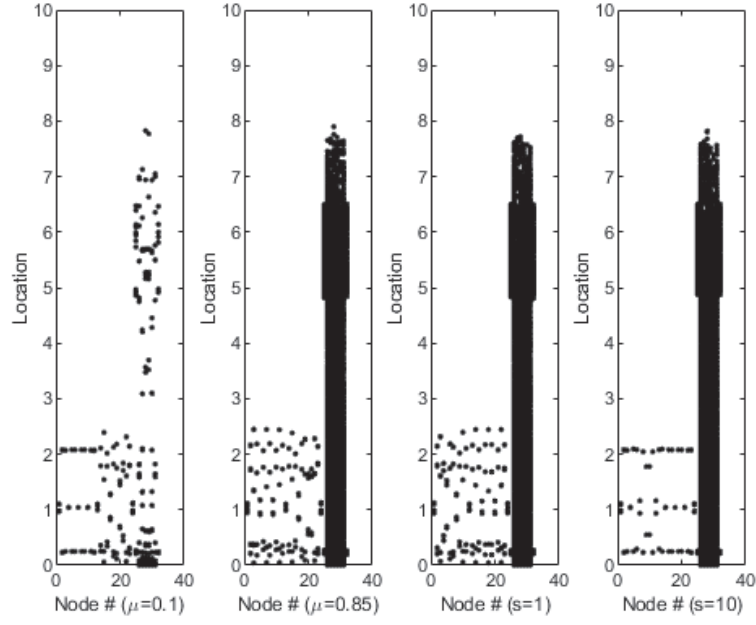


Figure 5.2: Node locations from iteration 2,000,000 to iteration 2,002,000 based off of the four sets provided in Table 5.1

cillators having an intrinsic growth rate $r = 3$ and the last 8 oscillators having an intrinsic growth rate of $r = 4.6$, we will change the connection strength b and plot the largest three LCEs for $b = 0$ to 0.5 . As before we let the system evolve for 2,000,000 iterations and use the next 50,000 iterations to calculate the LCEs. We are using seed $s = 1$ and our results can be seen in Figure 5.3.

In Figure 5.3, we see that the largest LCE value for most values of b is positive. When the connection strength is low from $b = 0.2$ to $b = 0.7$ the largest three LCE values are negative. For most values of b , we end up with both negative and positive LCE values. Recall from Figure 4.9 that we had many more values of b in which all three LCE values were negative. In Figure 4.11, for most values of b , all three LCE values were positive. This shows the dynamics of the system response

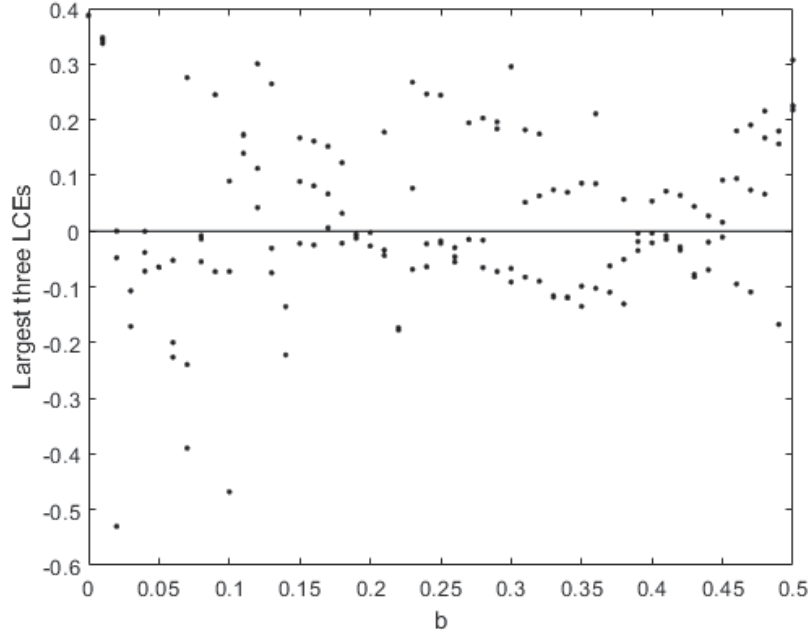


Figure 5.3: Largest 3 LCE values on a non-homogeneous ring for $b = 0$ to 0.5

as the intrinsic growth rate changes within the ring.

In this chapter, we explored a ring of non-identical oscillators where the first 24 nodes had intrinsic growth rate $r = 3$ and the last 8 nodes had intrinsic growth rate $r = 4.6$. We tested this ring using four different sets of initial conditions and we found that in all four sets, the LCEs were negative indicating a periodic system response. We conducted further analysis by plotting the node locations of all 32 nodes for each set of initial conditions. Finally, we wanted to see the response of the system when varying the connection strength b . Our results showed the the system behaved more closely to the system when $r = 4.6$ rather than when $r = 3$ for all 32 nodes. We found that for most values of b , we obtained a chaotic response.

Chapter 6

Connecting two rings of oscillators

In the first section, we will be connecting two identical rings of oscillators. We begin with two homogeneous rings of oscillators and connect a single node from ring X to a single node in ring Y . We will plot the evolution of a single node in this connected ring and determine whether the node exhibits a periodic or chaotic solution. We will then plot all of the LCE values in the system with two connected rings and observe the response.

In section two, we will observe the effects of coupling location on non-homogeneous rings of oscillators. We create ring X and ring Y with intrinsic growth rate $r = 3$ for the first 24 oscillators and $r = 4.6$ for the last 8 oscillators. In this section, we will observe four cases. In each case, four nodes in ring X are connected to four nodes in ring Y . In case 1, we will connect oscillators from the fourth quadrant of ring X to the fourth quadrant of ring Y . In case 2, we will connect oscillators from the second quadrant of ring X to the second quadrant of ring Y . In case 3, we will connect oscillators from the second quadrant of ring X to the fourth quadrant of ring Y . And in case 4, we will connect oscillators from the first quadrant of ring

X to the first quadrant of ring Y . We will then observe the node response of x_{12} and x_{27} and determine if their response is chaotic or periodic. We will also plot the LCE values for the system and show the time delayed response of the oscillators in the system.

6.1 Coupling two rings of oscillators through one common node

So far, we have worked with both homogeneous rings of oscillators and non-homogeneous rings of oscillators. In this section, we will be connecting two homogeneous rings of oscillators. We expand on Equation 2.1 and add a c component to it representing the connection strength of the connected nodes between the two rings X and Y and obtain the following iterative equations:

$$x_i(t+1) = bf(x_{i-1}(t), r_{i-1}) + af(x_i(t), r_i) + bf(x_{i+1}(t), r_{i+1}) + C(k, l)f(y_l(t), r_l) \quad (6.1)$$

$$y_j(t+1) = df(y_{j-1}(t), r_{j-1}) + cf(y_j(t), r_j) + df(y_{j+1}(t), r_{j+1}) + C(l, k)f(x_k(t), r_k). \quad (6.2)$$

Here, $C(k, l)$ and $C(l, k)$ represents the connection strength between coupled nodes. k is the node in ring X coupled with the l th node in ring Y . A visual representation of this system can be seen in Figure 6.1. In this section, we will focus on two homogeneous rings of oscillators coupled through a single node. We will let both rings have the same connection strength b but this does not have to be the case, as we will see in future sections.

We can generalize a model of two coupled rings such that, through the representation of the model, any node or nodes in ring X can be connected to any node or

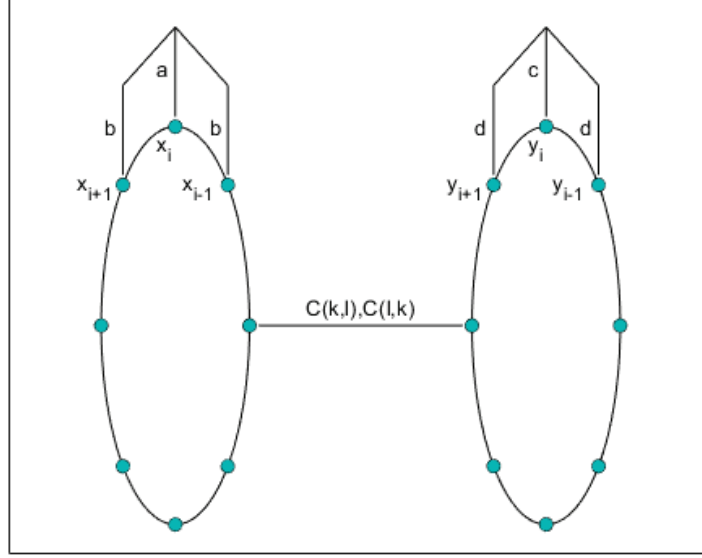


Figure 6.1: Coupled rings

nodes in ring Y . We will do this by treating each ring as a compartment. The rings do not have to be identical. The system of the coupled rings can be represented as

$$\begin{bmatrix} x(i+1) \\ y(i+1) \end{bmatrix} = \begin{bmatrix} A & C_{xy} \\ C_{yx} & B \end{bmatrix} \begin{bmatrix} f(x(i), r_x) \\ f(y(i), r_y) \end{bmatrix} \quad (6.3)$$

where

$$A = \begin{bmatrix} a & b & & b \\ b & a & b & \\ & b & a & b \\ & & \ddots & \\ & & & b & a \end{bmatrix} \quad \text{and} \quad B = \begin{bmatrix} c & d & & d \\ d & c & d & \\ & d & c & d \\ & & \ddots & \\ & & & d & c \end{bmatrix}$$

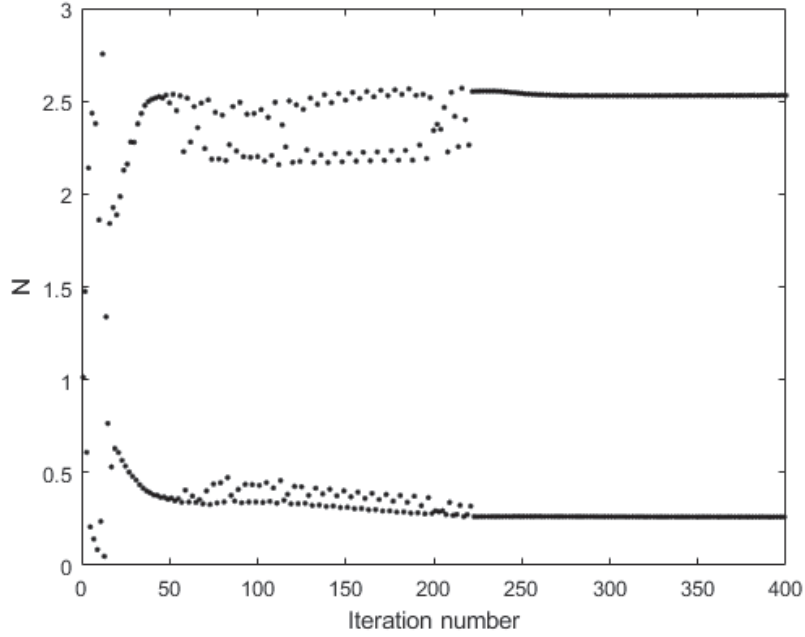


Figure 6.2: Evolution of the first node in ring X with $m = 2$ in coupled rings

Here, A and B are $n \times n$ matrices containing the connection strength of each node in their respective rings. C_{xy} and C_{yx} are also $n \times n$ matrices containing the connection strength of all coupled nodes.

As an example, consider two rings, X and Y , each containing 32 nodes with each node connected to its nearest neighbor. In addition, the first nodes of each ring are connected with connection strength $C = C_{xy}(1, 1) = C_{yx}(1, 1) = 0.2$. Just as in Figure 4.1, we view the response of the first node in ring X with intrinsic growth rate $r = 3$. We continue to use $s = 1$ for ring X but now we use $s = 2$ for ring Y . We continue to use $b = d = 0.2$. Recall that when $b = 0.2$, we obtained a periodic response from the uncoupled ring with periodicity 4.

Something interesting to note is that when $C = 0.2$, the response became periodic after only 220 iterations as opposed to becoming periodic after 1500 iterations

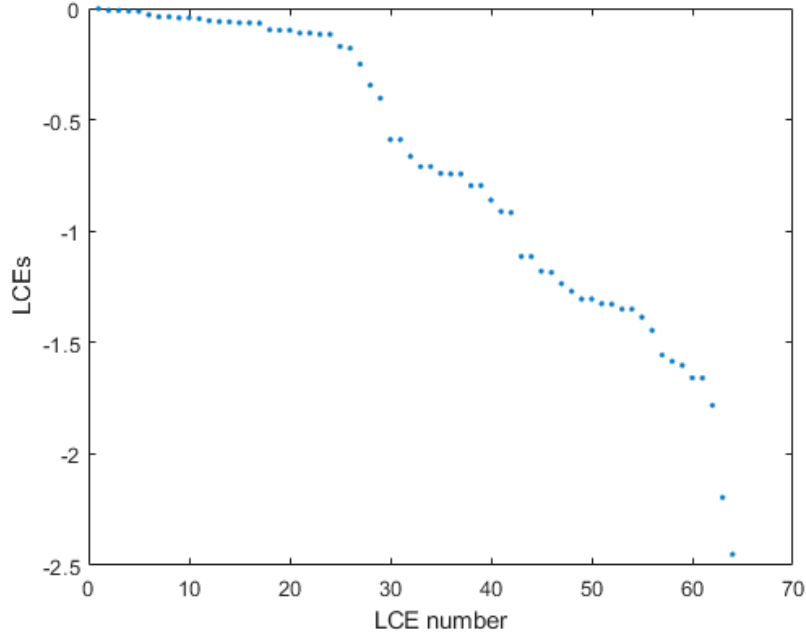


Figure 6.3: All LCE values when $s = 1$ for ring X and $s = 2$ for ring Y

in an uncoupled system.

We can calculate the LCEs for this coupled system after creating a map and tangent map of this system. The map of this system was created using Equation 6.3, and the tangent map was created by taking the Jacobian of the map. The tangent map is a $2n \times 2n$ matrix containing four compartments as mentioned above. To calculate the LCEs, we allow the system to evolve for 2,000,000 iterations and use the next 50,000 iterations to calculate the LCEs. We can see in Figure 6.3 that there are all negative value LCEs, except for the first LCE value which is very close to 0, and this agrees with Figure 6.2 which appears to have a periodic solution with periodicity two.

For the same system, we would like to view the largest three LCEs for varying values of C . Using the same system as in Figure 6.3, we generate the plot in Figure

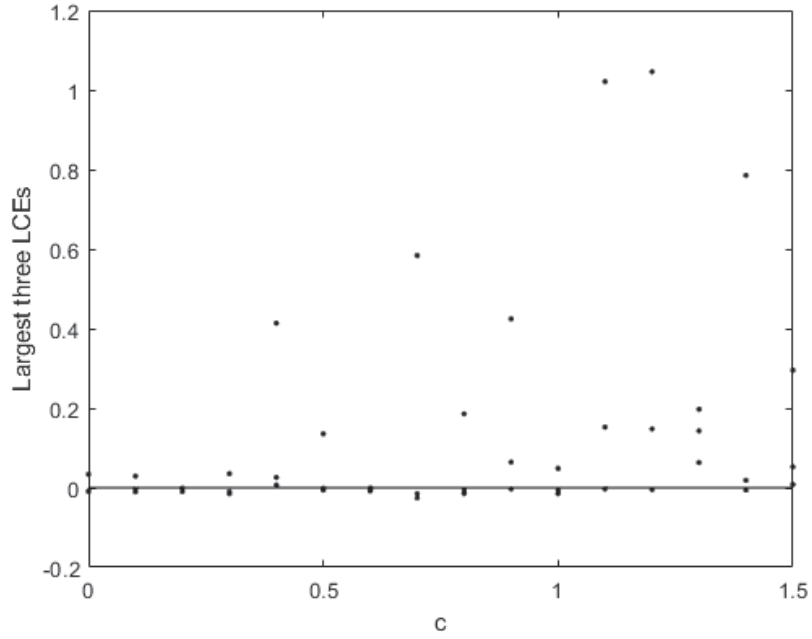


Figure 6.4: Largest three LCE values when $s = 1$ for ring X and $s = 2$ for ring Y for values of C from 0 to 1.5

6.4 which shows the largest three LCE values for $0 \leq C \leq 1.5$. Just as in Figure 6.3, the system was allowed to evolve for 2,000,000 iterations and we used the next 50,000 iterations to calculate the three largest LCEs for each value of C . We can see many values of C where the three largest LCEs are very close to 0. In these cases, further investigation is required to determine if the system is chaotic or periodic. However, there are some values of C such as $C = 1.3$ where there is clearly a chaotic response of the system.

6.2 Effects of coupling location on non-homogeneous rings

In this section, we will be coupling non-homogeneous rings of oscillators. We allow ring X to be identical to ring Y . That is, both rings will have each node connected to their nearest neighbor as in Equation 6.3 with connection strength $b = 0.2$. Again, we allow $a + mb = 1$ where $m = 2$ since we are connecting nearest neighbors. For both rings, we let the intrinsic growth rate $r = 3$ for the first 24 nodes and $r = 4.6$ for the last 8 nodes. Ring X and ring Y are 32 node rings with initial conditions calculated using seed $s = 1$ for ring X and seed $s = 2$ for ring Y .

There will be 4 cases in this section. In each case, we will be coupling 4 nodes from ring X to 4 nodes in ring Y . We split both rings into quadrants such that the first quadrant is given by nodes 1-8, the second quadrant is given by nodes 9-16, the third quadrant is given by nodes 17-24, and the fourth quadrant is given by nodes 25-32. We allow the coupling strength of the 4 chosen nodes to be $C_{xy} = C_{yx} = C = 0.65$.

For each case, there will be four subplots. The first subplot will be the evolution of the 12th and 27th nodes from iteration 2,000,001 to 2,000,050, a total of 50 points for each node. The second plot will contain the LCE values for the system. The last two plots will show the delayed response of the nodes using the same iterations as for the first subplot (2,000,0001 to 2,000,050).

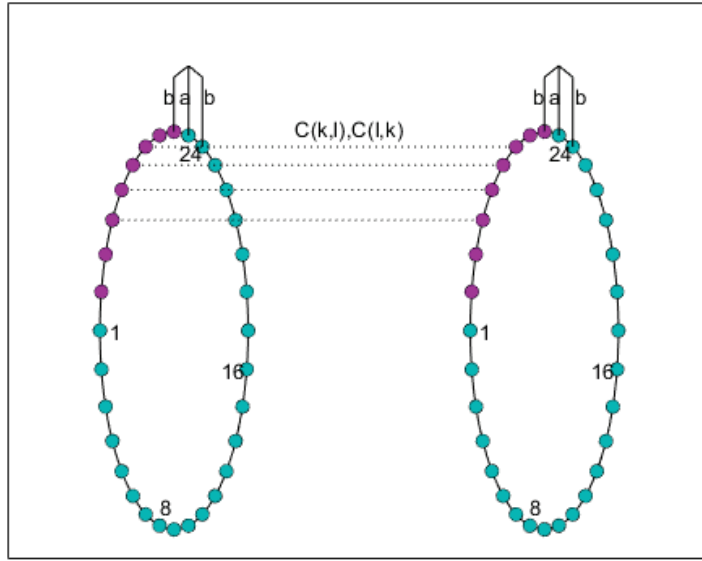
6.2.1 Case 1: Connecting oscillators from the fourth quadrant of ring X to the fourth quadrant of ring Y

In case one, we connect four nodes in quadrant four from ring X to four nodes in quadrant four in ring Y as seen in Figure 6.5(a). We couple x_{27} , x_{28} , x_{29} and x_{30} with y_{27} , y_{28} , y_{29} and y_{30} , respectively. The coupling strength used was $C_{xy} = C_{xy}(27, 27) = C_{xy}(28, 28) = C_{xy}(29, 29) = C_{xy}(30, 30) = 0.65$. All other nodes have a coupling strength of 0. Because all of the coupled nodes are in quadrant 4, the intrinsic growth rate for the coupled nodes is $r = 4.6$.

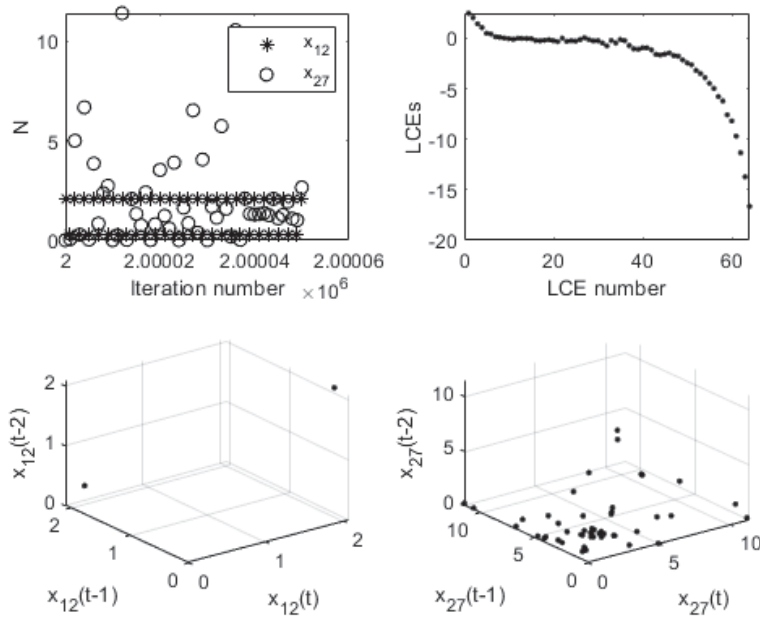
We can see from the first subplot in Figure 6.5(b) that x_{12} seems to be exhibiting periodic behavior with periodicity 2 while x_{27} seems to be exhibiting chaotic behavior. This indicates that the system will exhibit a chaotic response. This is further indicated by the second subplot because the largest LCEs are greater than 0, indicating a chaotic response. The last two subplots show the time delay of x_{12} and x_{27} for the system. Again, we see that x_{12} seems to show a periodic response while x_{27} is showing a chaotic response.

6.2.2 Case 2: Connecting oscillators from the second quadrant of ring X to the second quadrant of ring Y

In case one, we connected four nodes in quadrant four from ring X to four nodes in quadrant four in ring Y as seen in Figure 6.5(a). In case 2, we couple x_{11} , x_{12} , x_{13} and x_{14} with y_{11} , y_{12} , y_{13} and y_{14} , respectively. The coupling strength used was $C_{xy} = C_{xy}(11, 11) = C_{xy}(12, 12) = C_{xy}(13, 13) = C_{xy}(14, 14) = 0.65$. All other nodes had a coupling strength of 0. Because all of the coupled nodes were in quadrant 2, the intrinsic growth rate for the coupled nodes was $r = 3$.



(a)



(b)

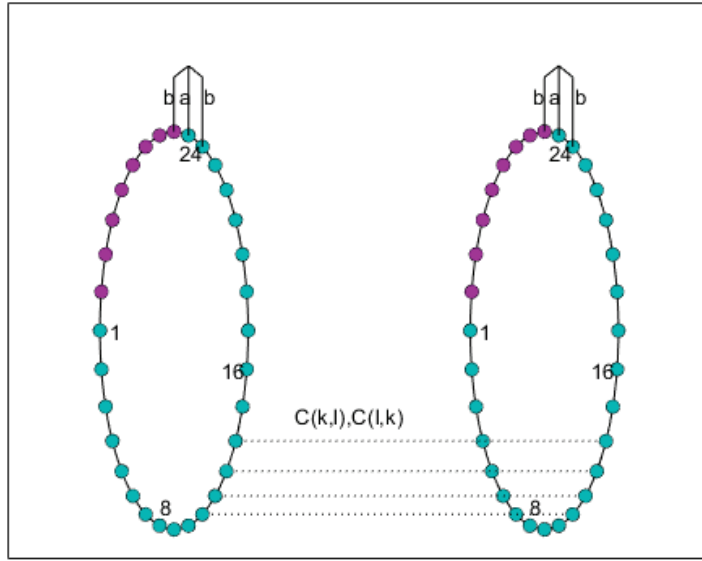
Figure 6.5: (a) Visualization of coupling for case 1 with $r = 3$ for quadrants 1-3 and $r = 4.6$ for quadrant 4. (b) Numerical results for case 1.

We can see from the first subplot in Figure 6.6(b) that x_{12} seems to be exhibiting periodic behavior with periodicity 2 while x_{27} seems to be exhibiting chaotic behavior. This indicates that the system will exhibit a chaotic response. This is further indicated by the second subplot because the largest LCEs are greater than 0, indicating a chaotic response. The last two subplots show the time delay of x_{12} and x_{27} for the system. Again, we see that x_{12} seems to show a periodic response while x_{27} is showing a chaotic response.

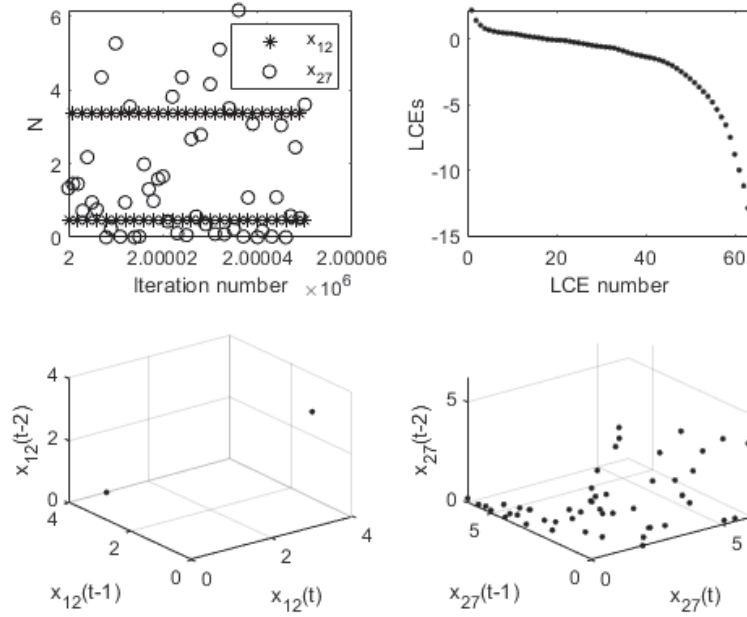
6.2.3 Case 3: Connecting oscillators from the second quadrant of ring X to the fourth quadrant of ring Y

In case 3, we couple x_{11} , x_{12} , x_{13} and x_{14} with y_{27} , y_{28} , y_{29} and y_{30} , respectively. The coupling strength used was $C_{xy} = C_{xy}(11, 27) = C_{xy}(12, 28) = C_{xy}(13, 29) = C_{xy}(14, 30) = 0.65$. All other nodes had a coupling strength of 0. Because all of the coupled nodes were in quadrant 2 for ring X and quadrant 4 in ring Y , the intrinsic growth rate for the coupled nodes was $r = 3$ in ring X and $r = 4.6$ in ring Y .

We can see from the first subplot in Figure 6.7(b) that x_{12} seems to be exhibiting periodic behavior with periodicity 2 while x_{27} seems to be exhibiting chaotic behavior. This indicates that the system will exhibit a chaotic response. This is further indicated by the second subplot because the largest LCEs are greater than 0, indicating a chaotic response. The last two subplots show the time delay of x_{12} and x_{27} for the system. Again, we see that x_{12} seems to show a periodic response while x_{27} is showing a chaotic response.

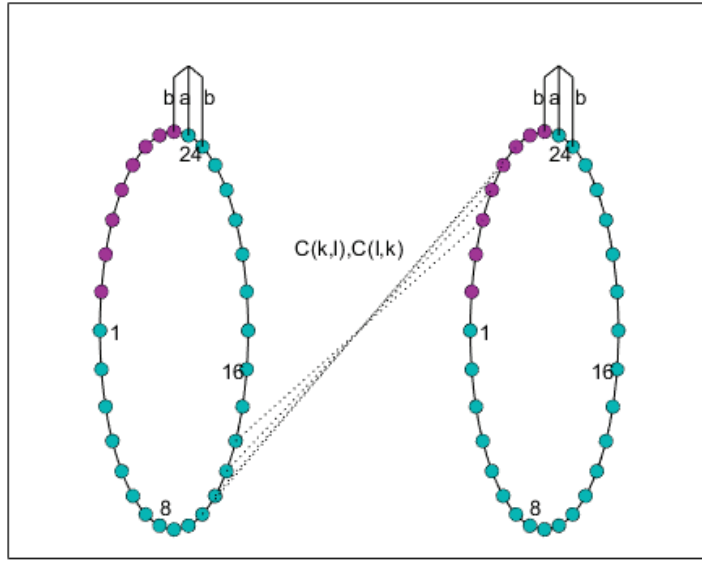


(a)

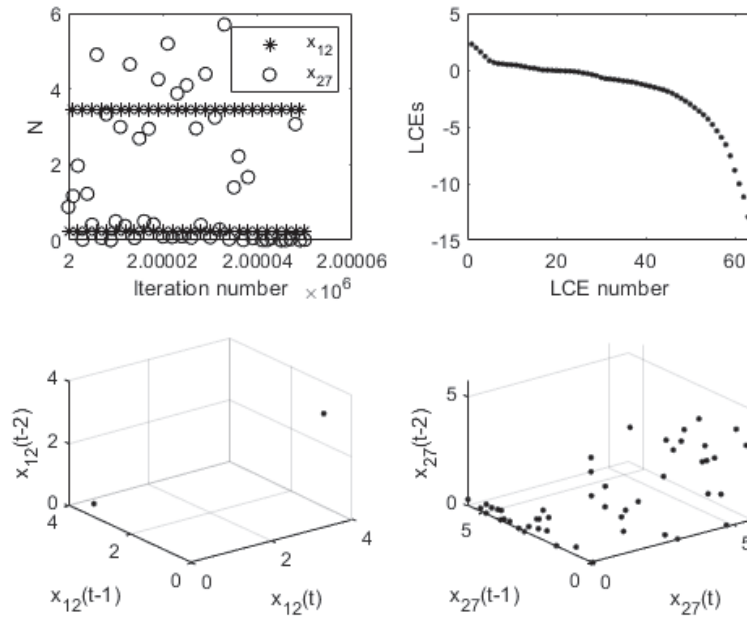


(b)

Figure 6.6: (a) Visualization of coupling for case 2 with $r = 3$ for quadrants 1-3 and $r = 4.6$ for quadrant 4. (b) Numerical results for case 1.



(a)



(b)

Figure 6.7: (a) Visualization of coupling for case 3 with $r = 3$ for quadrants 1-3 and $r = 4.6$ for quadrant 4. (b) Numerical results for case 1.

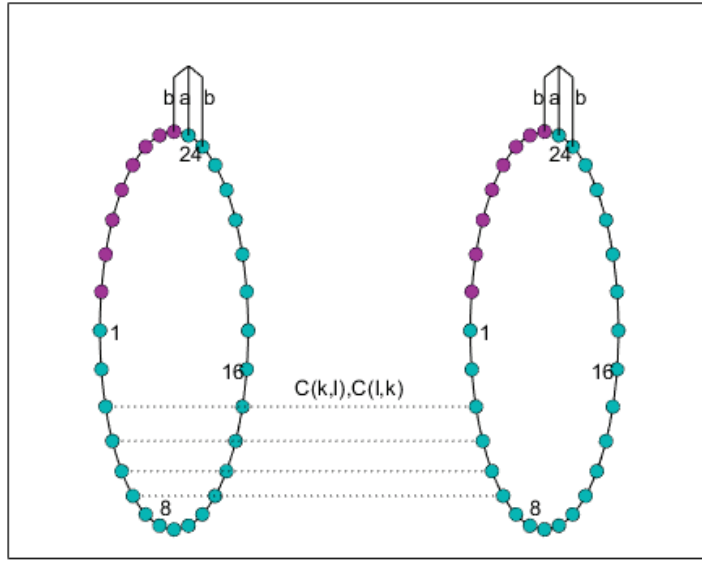
6.2.4 Case 4: Connecting oscillators from the first quadrant of ring X to the first quadrant of ring Y

In case 4, we couple x_3, x_4, x_5 and x_6 with y_3, y_4, y_5 and y_6 , respectively. The coupling strength used was $C_{xy} = C_{xy}(3, 3) = C_{xy}(4, 4) = C_{xy}(5, 5) = C_{xy}(6, 6) = 0.65$. All other nodes had a coupling strength of 0. Because all of the coupled nodes were in quadrant 1, the intrinsic growth rate for the coupled nodes was $r = 3$.

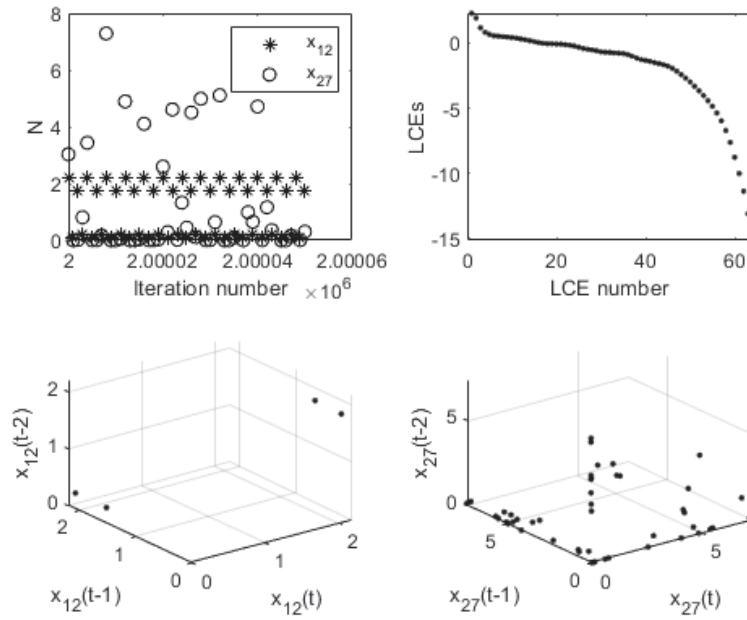
We can see from the first subplot in Figure 6.8(b) that x_{12} seems to be exhibiting periodic behavior with periodicity 4 while x_{27} seems to be exhibiting chaotic behavior. This indicates that the system will exhibit a chaotic response. This is further indicated by the second subplot because the largest LCEs are greater than 0, indicating a chaotic response. The last two subplots show the time delay of x_{12} and x_{27} for the system. Again, we see that x_{12} seems to show a periodic response while x_{27} is showing a chaotic response.

In the first section, we connected two identical rings of oscillators. We began with two homogeneous rings of oscillators and connected a single node from ring X to a single node in ring Y . We plotted the evolution of a single node in this connected ring and the node exhibited a periodic response with periodicity two. We then plotted all of the LCE values in the system with two connected rings and found them to be negative or very close to zero.

In section two, we observed the effects of coupling location on non-homogeneous rings of oscillators. Both ring X and ring Y had intrinsic growth rate $r = 3$ for the first 24 oscillators and $r = 4.6$ for the last 8 oscillators. In this section, we observed four cases. In each case, four nodes in ring X were connected to four nodes in ring Y . In case 1, we connected oscillators from the fourth quadrant of ring X to the fourth quadrant of ring Y . We observed that node x_{12} in ring X exhibited a periodic



(a)



(b)

Figure 6.8: (a) Visualization of coupling for case 4 with $r = 3$ for quadrants 1-3 and $r = 4.6$ for quadrant 4. (b) Numerical results for case 1.

response with periodicity two and x_{27} exhibited a chaotic response. The positive LCEs in this system indicated that the system had a chaotic response. While case 2 and 3 had different coupling locations, case 2 having a coupling from quadrant 2 of ring X to quadrant 2 of ring Y , and case 3 having a coupling from quadrant 2 of ring X to quadrant 4 of ring Y , the results appeared to be similar to the first case. The node response of x_{12} appeared to be periodic with periodicity two while the node response of x_{27} appeared to be chaotic. There were also positive LCE responses in case 2 and 3 indicating that the system exhibited chaotic behavior. In case 4, we coupled nodes from quadrant 1 in ring X to quadrant 1 in ring Y . The results were similar to the first three cases but this time x_{12} exhibited a periodic response with periodicity four.

Chapter 7

Conclusion

In chapter two, we introduced the Ricker model and its bifurcation plot. We observed values of the intrinsic growth rate r for which we obtained periodic solutions. We also observed regions of the bifurcation plot for which we obtained chaotic solutions.

In chapter three, we introduced Lyapunov Characteristic Exponents which can measure perturbations of a dynamical system. Negative LCE values indicate that the system is likely periodic while positive LCE values indicate a chaotic response.

In the first section of chapter four, we began our analysis by observing the evolution of a single node in a ring with 32 oscillators with each oscillator connected to its nearest neighbor. We found that the observed node exhibited a chaotic response that eventually turned periodic with a periodicity of four. However, when we conducted this analysis with the same initial conditions except without connecting the nearest neighbors, we found that the system remained chaotic, even after 2,000,000 iterations. In order to determine if the system was indeed chaotic, we developed a map and tangent map for use in calculating LCEs and found that the

unconnected system was chaotic while the system with each node connected to its nearest neighbor was periodic.

In section two of chapter four, explored the effects of changing the initial conditions by changing the seed values. We used a system where each node is connected to its nearest neighbor and calculated the largest 5 LCEs with initial conditions produced using six different seed values. For each seed chosen, we found that the LCE values were different, but in all six cases, the largest five LCEs remained negative and the system for each case had a periodicity of four. We could further explore these results to see if we can find a system that is periodic with certain seed values and chaotic with others. Because the system observed was periodic, with each node having periodicity four, there were $32 \times 4 = 128$ possible solutions for each seed value observed. We arranged the node responses from smallest to largest to make a comparison between the node responses of each system. We found that changing the initial conditions by using different seed values generated different solutions for each system.

In section three of chapter four, we observed a system with a symmetric response. The system that we observed appeared to have a two period solution, but it was actually a four period solution that was symmetric. We were able to show the symmetry by plotting the periodic solution in a ring and observing which nodes had the same node response. We found that all of the seed values tested produced either 64 or 128 possible solutions depending on whether or not the system was symmetric.

In section four of chapter four, we observed the effects of changing the connection strength, b , in a ring with 32 connected nodes, each node connected to its nearest neighbor. We had already explored the system response when the connec-

tion strength was $b = 0.2$. We then tested the response of the connected ring by varying b from 0 to 0.5 and observed the largest 3 LCEs produced for each value of b . We found that in a connected ring for the initial conditions used, specifically $r = 3$, that most of the values of b produced a periodic response. We then set $r = 4.6$ and found the largest 3 LCEs for each value of b when b was varied from 0 and 0.5. With $r = 4.6$ in a system where each node is connected to its nearest neighbor, we found that most of the LCEs were positive indicating a chaotic response.

In section five of chapter four, we created a ring with 32 nodes, each node connected to its nearest two neighbors. We observed the evolution of a single node with the intrinsic growth rate $r = 4.6$. This value of the intrinsic growth rate was used because we had previously found that for this node, given the initial conditions, in a system where only the nearest neighbors were connected, there was a chaotic response. By connecting more nodes in the system, we were able to turn a response that was previously chaotic into a periodic response. In this paper, we observed results of rings of oscillators in a disconnected system, a ring with nodes connected to their nearest neighbors, and a ring with nodes connected to their nearest two neighbors. It seems as though the more connected the system is, the more likely it is for the node responses to become periodic. Further analysis would include connecting more nodes, including a ring that is completely connected. Such a ring was not tested in this paper because it was too computationally expensive.

In chapter five, we explored a ring of non-identical oscillators where the first 24 nodes had intrinsic growth rate $r = 3$ and the last 8 nodes had intrinsic growth rate $r = 4.6$. We tested this ring using four different sets of initial conditions and we found that in all four sets, the LCEs were negative indicating a periodic system response. We conducted further analysis by plotting the node locations of all 32

nodes for each set of initial conditions. Finally, we wanted to see the response of the system when varying the connection strength b . Our results showed that the system behaved more closely to the system when $r = 4.6$ rather than the system when $r = 3$ for all 32 nodes. We found that for most values of b , we obtained a chaotic response.

In the first section of chapter 6, we connected two identical rings of oscillators. We began with two homogeneous rings of oscillators and connected a single node from ring X to a single node in ring Y . We plotted the evolution of a single node in this connected ring and the node exhibited a periodic response with periodicity two. We then plotted all of the LCE values in the system with two connected rings and found them to be negative or very close to zero.

In section two of chapter 6, we observed the effects of coupling location on non-homogeneous rings of oscillators. Both ring X and ring Y had intrinsic growth rate $r = 3$ for the first 24 oscillators and $r = 4.6$ for the last 8 oscillators. In this section, we observed four cases. In each case, four nodes in ring X were connected to four nodes in ring Y . In case 1, we connected oscillators from the fourth quadrant of ring X to the fourth quadrant of ring Y . We observed that node x_{12} in ring X exhibited a periodic response with periodicity two and x_{27} exhibited a chaotic response. The positive LCEs in this system indicated that the system had a chaotic response. While case 2 and 3 had different coupling locations, case 2 having a coupling from quadrant 2 of ring X to quadrant 2 of ring Y , and case 3 having a coupling from quadrant 2 of ring X to quadrant 4 of ring Y , the results appeared to be similar to the first case. The node response of x_{12} appeared to be periodic with periodicity two while the node response of x_{27} appeared to be chaotic. There were also positive LCE responses in case 2 and 3 indicating that the system exhibited chaotic behavior. In

case 4, we coupled nodes from quadrant 1 in ring X to quadrant 1 in ring Y . The results were similar to the first three cases but this time x_{12} exhibited a periodic response with periodicity four.

There were several notable results in this paper. The first notable result stems from plotting the time evolution of a single oscillator. We found that an oscillator that appeared chaotic can become periodic after allowing the oscillator to evolve. Not only can the node response become periodic, but the transition into a periodic solution occurs within very few iterations. Another notable result in this paper were the effects initial conditions had on the response of the system. By plotting the response of all oscillators using various seed values, we were able to observe that changing the initial conditions changes the solution. One of the most fascinating results came from connecting oscillators to their nearest neighbors in a ring. We found that the node responses can become periodic when connected to their nearest neighbors, despite the chaotic nature of individual oscillators. Lastly, we were unable to find coupled rings of oscillators that exhibited periodic global behavior. Further investigation will need to be done in order to find coupled rings of oscillators that do not exhibit a chaotic global response using the Ricker model.

There is still much more analysis that can be done in exploring rings of non-homogeneous oscillators. We explored a small subset of all the possible combinations that could have been explored with these rings. To name a few, we explored rings of oscillators with 32 oscillators in each ring. We could have explored the effects of changing the number of oscillators in each ring and varying the initial conditions given the new ring with a different number of oscillators. One of the limitations in this paper is that we were not able to analyze a completely connected ring due to computational speed. Other methods would be needed such as parallel

computing in order to bring down the computation speed enough to do analysis on more complicated rings. It is the hope that the theory and analysis done in this paper could be used in future real-life applications.

Bibliography

- [1] Hubertus F. von Bremen, Firdaus E. Udwadia, *Computational explorations into the dynamics of rings of coupled oscillators*, Department of Aerospace and Mechanical Engineering, University of Southern California, 55-85, 2002.
- [2] Hubertus F. von Bremen, Firdaus E. Udwadia, Wlodek Proskurowski, *An efficient QR based method for the computation of Lyapunov exponents*, Phys. D, 101(1-2):1-16, 1997.
- [3] W.E. Ricker, *Stock and Recruitment*, Journal of the Fisheries Research Board of Canada, Vol. 11, No.5:pp. 559-623, 1954.
- [4] Charalampos Skokos, *The Lyapunov Characteristic Exponents and Their Computation*, Springer Berlin Heidelberg, 2010.
- [5] Bing Jia, Huanguang Gu, Li Li, Xiaoyan Zhao, *Dynamics of period-doubling bifurcation to chaos in the spontaneous neural firing patterns*, Cognitive Neurodynamics, 2012.
- [6] Xingyuan Wang, Jianfeng Zhao, *An improved key agreement protocol based on chaos*, Commun. Nonlinear Sci. Numer. Simul., 2012.

- [7] Ulrich Nehmzow, Keith Walker, *Quantitative description of robo-environment interaction using chaos theory*, Robotics and Autonomous Systems, 2005.
- [8] A. Morbidelli, *Chaotic diffusion in celestial mechanics*, Regular and Chaotic Dynamics, 2001.
- [9] Ake Brannstrom, David Sumpter, *The role of competition and clustering in population dynamics*, Proceedings of the Royal Society B: Biological Sciences, 2005.
- [10] Swarup Poria, Mohammad Ali Khan, Mayurakshi Nag, *Spatiotemporal synchronization of coupled Ricker maps over a complex network*, Physica Scripta, 2013.
- [11] Jan Philipp Pade, Leonhard Lucken, Serhiy Yanchuk, *The dynamical impact of a shortcut in unidirectionally coupled rings of oscillators*, Humboldt-University of Berlin, Institute of Mathematics, 2015.

Appendices

Appendix A

MATLAB code for figures

Listing A.1: Figure 2.2

```
1  %Initial Conditions
2  T=zeros(1000000, 2); %length of r * length of i
3  count=1;
4  n=1;
5  s=1;
6
7  for r=1:.01:4.5
8      %Initial Conditions
9      rand('seed', s)
10     N = rand(1,n)+.5;
11     for i=0:1250
12         N=N*exp(r*(1-N));
13         if i>1000 %Letting N evolve for 750 iterations before taking values
14             T(count,:)= [r N];
15             count=count+1;
16         end
17     end
18 end
19
20 %Getting rid of extra T values
21 T(T(:,1)==0, :)=[];
22
```



```

23 %Plotting figure
24 figure(1)
25 plot(T(:,1), T(:,2), '.', 'color', 'black');
26 xlabel('r')
27 ylabel('N_t')

```

Listing A.2: Figure 4.1

```

1 %% Initial conditions
2 iteration=1000;
3 b=0.2;
4 r=3;
5 n=32; %nodes
6 s=1; %seed
7 N_span=999; %frame of plot
8 node = 2;
9
10 %% Finding x
11 [ N ] = map_ricker_nearestNeighbor ( iteration, b, r, n, s );
12
13 %% Plot figure
14 figure
15 plot(iteration-N_span:iteration, N(iteration-N_span:iteration,node), '.', ...
      'color', 'black')
16 xlabel('Iteration number')
17 ylabel('N')

```

Listing A.3: Figure 4.1

```

1  %% Initial conditions
2  iteration=1000;
3  b=0.2;
4  r=3;
5  n=32; %nodes
6  s=1; %seed
7  Nspan=999; %frame of plot
8  node = 2;
9
10 %% Finding x
11 [ N ] = map_ricker_nearestNeighbor ( iteration, b, r, n, s );
12
13 %% Plot figure
14 figure
15 plot(iteration-Nspan:iteration, N(iteration-Nspan:iteration,node), '.', ...
      'color', 'black')
16 xlabel('Iteration number')
17 ylabel('N')

```

Listing A.4: Table 4.1

```

1  map='map_ricker_nearestNeighbor';
2  tanmap='tanmap_ricker_nearestNeighbor';
3  iteration=2050000;
4  lce_iteration=50000;
5  b=0.2;
6  r=3;
7  n=32;
8
9  S=[1;5;10;14;16;20];
10 T=cell(1,length(S));
11 for i=1:length(S)
12     s=S(i);
13     [ LCEvector ] = LCE( map, tanmap, iteration, lce_iteration, b, r, n, s );
14     T{1,i} = maxk(LCEvector, 5);
15 end

```

Listing A.5: Figure 4.4

```

1  %% seed is 1
2  %initial conditions
3  iteration=200000;
4  b=.2;
5  r=3;
6  n=32; %nodes
7  s=1; %seed
8
9  %Creates the table x which will store all x values of the ringed oscillator
10 [ x ] = map_ricker_nearestNeighbor ( iteration, b, r, n, s );
11
12 %Manipulating to create an array
13 x=x(end-3:end, :);
14 x=x(:);
15 x=sortrows(x);
16 index=1:length(x);
17
18 figure(6)
19 plot(index, x, 'sq')
20 hold on;
21 length(unique(round(x,6)))
22
23 %% seed is 14
24 %initial conditions
25 iteration=200000;
26 b=.2;
27 r=3;
28 n=32; %nodes
29 s=14; %seed
30
31 %Creates the table x which will store all x values of the ringed oscillator
32 [ x ] = map_ricker_nearestNeighbor ( iteration, b, r, n, s );
33
34 %Manipulating to create an array
35 x=x(end-3:end, :);
36 x=x(:);
37 x=sortrows(x);

```

```

38 index=1:length(x);
39
40 plot(index, x, 'd')
41 length(unique(round(x,6)))
42
43 %% seed is 16
44 %initial conditions
45 iteration=200000;
46 b=.2;
47 r=3;
48 n=32; %nodes
49 s=16; %seed
50
51 %Creates the table x which will store all x values of the ringed oscillator
52 [ x ] = map_ricker_nearestNeighbor ( iteration, b, r, n, s );
53
54 %Manipulating to create an array
55 x=x(end-3:end, :);
56 x=x(:);
57 x=sortrows(x);
58 index=1:length(x);
59
60 plot(index, x, 'o')
61 length(unique(round(x,6)))
62 legend( 'seed=1', 'seed=14', 'seed=16', 'location', 'southeast' )

```

Listing A.6: Figure 4.5

```
1  %initial conditions
2  iteration=2000000;
3  b=.2;
4  r=3;
5  n=32; %nodes
6  s=29; %seed
7
8  %Creates the table x which will store all x values of the ringed oscillator
9  [ x ] = map_ricker_nearestNeighbor ( iteration, b, r, n, s );
10
11 %Plot of n vs x
12 for i=1:n
13     x_node=x(end-x.span:end, i);
14
15     figure(7)
16     plot(ones(length(x_node), 1)*i, x_node, '.', 'color', 'black')
17     hold on;
18 end
19
20 xlabel('Node Number')
21 ylabel('N-value')
```

Listing A.7: Figure 4.8

```

1  %% Plot Ellipse
2
3  a=4; % horizontal radius
4  b=.8; % vertical radius
5  x0=0; % x0,y0 ellipse centre coordinates
6  y0=0;
7  t=-pi:0.01:pi;
8  x=x0+a*cos(t);
9  y=y0+b*sin(t);
10
11 figure(12)
12 subplot(2,2,1), plot(x,y, 'color', 'black')
13 xlim([-a-1 a+1])
14 ylim([-a-1 a+1])
15 title('iteration = 2,000,000')
16 set(gca,'XTick',[], 'YTick', [])
17 hold on;
18
19 subplot(2,2,2), plot(x,y, 'color', 'black')
20 xlim([-a-1 a+1])
21 ylim([-a-1 a+1])
22 title('iteration = 2,000,001')
23 set(gca,'XTick',[], 'YTick', [])
24 hold on;
25
26 subplot(2,2,3), plot(x,y, 'color', 'black')
27 xlim([-a-1 a+1])
28 ylim([-a-1 a+1])
29 title('iteration = 2,000,002')
30 set(gca,'XTick',[], 'YTick', [])
31 hold on;
32
33 subplot(2,2,4), plot(x,y, 'color', 'black')
34 xlim([-a-1 a+1])
35 ylim([-a-1 a+1])
36 title('iteration = 2,000,003')
37 set(gca,'XTick',[], 'YTick', [])

```

```

38 hold on;
39
40 %% Plot dots
41
42 t_dot=-pi:pi/16:pi;
43 x_dot=x0+a*cos(t_dot);
44 y_dot=y0+b*sin(t_dot);
45
46 x_dot=x_dot';
47 y_dot=y_dot';
48
49 %Making this the correct number of rows
50 x_dot(end)=[];
51 y_dot(end)=[];
52
53 subplot(2,2,1), plot(x_dot, y_dot, 'o', 'color', 'black') %dots
54 subplot(2,2,1), scatter(x_dot([8 24]), y_dot([8 24]), 'filled', 'o') %fill 8th ...
    and 24th dots
55 text(x_dot(7:9), y_dot(7:9)-.6, {'7', '8', '9'})
56
57 subplot(2,2,2), plot(x_dot, y_dot, 'o', 'color', 'black') %dots
58 subplot(2,2,2), scatter(x_dot([8 24]), y_dot([8 24]), 'filled', 'o') %fill 8th ...
    and 24th dots
59 text(x_dot(7:9), y_dot(7:9)-.6, {'7', '8', '9'})
60
61 subplot(2,2,3), plot(x_dot, y_dot, 'o', 'color', 'black') %dots
62 subplot(2,2,3), scatter(x_dot([8 24]), y_dot([8 24]), 'filled', 'o') %fill 8th ...
    and 24th dots
63 text(x_dot(7:9), y_dot(7:9)-.6, {'7', '8', '9'})
64
65 subplot(2,2,4), plot(x_dot, y_dot, 'o', 'color', 'black') %dots
66 subplot(2,2,4), scatter(x_dot([8 24]), y_dot([8 24]), 'filled', 'o') %fill 8th ...
    and 24th dots
67 text(x_dot(7:9), y_dot(7:9)-.6, {'7', '8', '9'})
68
69 %% Now plot the diamonds
70
71 %initial conditions

```

```

72 iteration=2000003;
73 b=.2;
74 r=3;
75 n=32; %nodes
76 s=29; %seed
77
78 %Creates the table x which will store all x values of the ringed oscillator
79 [ x ] = map_ricker_nearestNeighbor ( iteration, b, r, n, s );
80
81 %% Preparing to make the ring graph
82 x=x(end-3:end, :);
83
84 for i=1:size(x,1)
85
86     y_dia=x(i, :);
87     y_dia=y_dot+y_dia;
88
89     subplot(2,2,i), scatter(x_dot, y_dia, 'filled', 'd')
90     subplot(2,2,i), plot(x_dot, y_dia, '-', 'color', 'black')
91     subplot(2,2,i), plot([x_dot(1);x_dot(end)], [y_dia(1);y_dia(end)], '-', ...
92         'color', 'black')
93
94     for j=1:length(x_dot)
95
96         line([x_dot(j) x_dot(j)], [y_dot(j) y_dia(j)], 'color', 'black')
97     end
98 end

```


Listing A.8: Figure 4.9

```

1  %Initial Conditions
2  map='map_ricker_nearestNeighbor';
3  tanmap='tanmap_ricker_nearestNeighbor';
4  iteration=2000000;
5  lce_iteration=50000;
6  r=3; %unused in this case
7  n=32; %nodes
8  s=1; %seed
9
10 for b=0:.1:0.5
11
12     %Find LCEs
13     LCEvector = LCE ( map, tanmap, iteration, lce_iteration, b, r, n, s );
14
15     %Plot Figure
16     figure(10)
17     y_plot=maxk(LCEvector,3);
18     x_plot=[b;b;b];
19     plot(x_plot, y_plot, 'black. ');
20     hold on;
21 end
22
23 %plot line
24 xline=[0 .5];
25 yline=[0 0];
26 plot(xline, yline, 'color', 'black');
27 xlabel('b');
28 ylabel('Largest three LCEs');

```

Listing A.9: Figure 5.1: Nonhomogeneous map

```

1 function [ N ] = map_ricker_nearestNeighbor_nha ( iteration, b, r, n, r )
2 %% Generate initial value for x
3 N=zeros(iteration, n); % Initial conditions
4 mu=.1;
5 v=5;
6 a=1-2*b;
7
8 for j=1:n
9     N(1,j)=mu*sin((v*pi*(j-1))/(n-1))+1;
10 end
11
12 %% Map of Ricker connecting to nearest neighbor
13 for i=2:iteration
14     for j=1:n
15
16         if j<24
17             r=3;
18         else
19             r=4.6;
20         end
21
22         if j==1
23             N(i,1)=b*(N(i-1,n)*exp(r*(1-N(i-1,n))))...
24                 +a*(N(i-1,1)*exp(r*(1-N(i-1,1))))...
25                 +b*(N(i-1,2)*exp(r*(1-N(i-1,2))));
26         elseif j==n
27             N(i,n)=b*(N(i-1,n-1)*exp(r*(1-N(i-1,n-1))))...
28                 +a*(N(i-1,n)*exp(r*(1-N(i-1,n))))...
29                 +b*(N(i-1,1)*exp(r*(1-N(i-1,1))));
30         else
31             N(i,j)=b*(N(i-1,j-1)*exp(r*(1-N(i-1,j-1))))...
32                 +a*(N(i-1,j)*exp(r*(1-N(i-1,j))))...
33                 +b*(N(i-1,j+1)*exp(r*(1-N(i-1,j+1))));
34         end
35     end
36 end

```

Listing A.10: Figure 5.1: Nonhomogeneous tangent map

```

1 function [ tanmap ] = tanmap-ricker.nearestNeighbor_nha ( Ni, b, r, n )
2 %% Initial conditions
3
4 a=1-2*b;
5 tanmap=zeros(n);
6
7 %% Tangent map
8 for i=1:n
9     if i≤24
10         r=3;
11     else
12         r=4.6;
13     end
14
15     if i==1
16         tanmap(1,n)=b*(exp(r*(1-Ni(n))))*(1-r*Ni(n));
17         tanmap(1,1)=a*(exp(r*(1-Ni(1))))*(1-r*Ni(1));
18         tanmap(1,2)=b*(exp(r*(1-Ni(2))))*(1-r*Ni(2));
19     elseif i==n
20         tanmap(n,n-1)=b*(exp(r*(1-Ni(n-1))))*(1-r*Ni(n-1));
21         tanmap(n,n)=a*(exp(r*(1-Ni(n))))*(1-r*Ni(n));
22         tanmap(n,1)=b*(exp(r*(1-Ni(1))))*(1-r*Ni(1));
23     else
24         tanmap(i,i-1)=b*(exp(r*(1-Ni(i-1))))*(1-r*Ni(i-1));
25         tanmap(i,i)=a*(exp(r*(1-Ni(i))))*(1-r*Ni(i));
26         tanmap(i,i+1)=b*(exp(r*(1-Ni(i+1))))*(1-r*Ni(i+1));
27     end
28 end

```

Listing A.11: Figure 5.2

```

1  %% Fig a
2  iteration=2002000;
3  b=.2;
4  r=0; %unused
5  n=32; %nodes
6  s=0; %unused
7
8  [ N ] = map_ricker_nearestNeighbor_nha ( iteration, b, r, n, s );
9
10 for i=1:n
11
12     figure(15)
13     subplot(1,4,1), plot(ones(2001,1)*i, N(2000000:2002000, i), '.', 'color', ...
14         'black');
15     hold on;
16 end
17 xlim([0 40]);
18 ylim([0 10]);
19 xlabel('Node # (\mu=0.1)');
20 ylabel('Location');
21
22 %% Fig b
23 iteration=2002000;
24 b=.2;
25 r=0; %unused
26 n=32; %nodes
27 s=0; %unused
28
29 [ N ] = map_ricker_nearestNeighbor_nhb ( iteration, b, r, n, s );
30
31 for i=1:n
32
33     figure(15)
34     subplot(1,4,2), plot(ones(2001,1)*i, N(2000000:2002000, i), '.', 'color', ...
35         'black');
36     hold on;

```

```

36 end
37
38 xlim([0 40]);
39 ylim([0 10]);
40 xlabel('Node # (\mu=0.85)');
41 ylabel('Location');
42
43 %% Fig c
44 iteration=2002000;
45 b=.2;
46 r=0; %unused
47 n=32;
48 s=1;
49
50 [ N ] = map_ricker_nearestNeighbor_nhc ( iteration, b, r, n, s );
51
52 for i=1:n
53
54     figure(15)
55     subplot(1,4,3), plot(ones(2001,1)*i, N(2000000:2002000, i), '.', 'color', ...
        'black');
56     hold on;
57 end
58
59 xlim([0 40]);
60 ylim([0 10]);
61 xlabel('Node # (s=1)');
62 ylabel('Location');
63
64 %% Fig d
65 iteration=2002000;
66 b=.2;
67 r=3; %unused
68 n=32;
69 s=10;
70
71 [ N ] = map_ricker_nearestNeighbor_nhc ( iteration, b, r, n, s );
72

```

```
73 for i=1:n
74
75     figure(15)
76     subplot(1,4,4), plot(ones(2001,1)*i, N(2000000:2002000, i), '.', 'color', ...
        'black');
77     hold on;
78 end
79
80 xlim([0 40]);
81 ylim([0 10]);
82 xlabel('Node # (s=10)');
83 ylabel('Location');
```

Listing A.12: Figure 6.1: Coupled map

```

1 function [ N ] = map_ricker_nearestNeighbor_coupled ( iteration, b, r, n, s, c )
2 % Initial conditions for first X
3 N1=zeros(iteration, n);
4 rand('seed', s)
5 N1(1,:) = rand(1,n)+.5;
6
7 % Initial conditions for second Y
8 s = s+1;
9 N2=zeros(iteration, n);
10 rand('seed', s)
11 N2(1,:) = rand(1,n)+.5;
12
13 a=1-2*b;
14
15 for i=2:iteration      % Map of Ricker connecting to nearest neighbor
16     for j=1:n
17         if j==1
18             %Ring X
19             N1(i,1)=b*(N1(i-1,n)*exp(r*(1-N1(i-1,n))))...
20                 +a*(N1(i-1,1)*exp(r*(1-N1(i-1,1))))...
21                 +b*(N1(i-1,2)*exp(r*(1-N1(i-1,2))))...
22                 +c*(N2(i-1,1)*exp(r*(1-N2(i-1,1))));
23             %Ring Y
24             N2(i,1)=b*(N2(i-1,n)*exp(r*(1-N2(i-1,n))))...
25                 +a*(N2(i-1,1)*exp(r*(1-N2(i-1,1))))...
26                 +b*(N2(i-1,2)*exp(r*(1-N2(i-1,2))))...
27                 +c*(N1(i-1,1)*exp(r*(1-N1(i-1,1))));
28         elseif j==n
29             %Ring X
30             N1(i,n)=b*(N1(i-1,n-1)*exp(r*(1-N1(i-1,n-1))))...
31                 +a*(N1(i-1,n)*exp(r*(1-N1(i-1,n))))...
32                 +b*(N1(i-1,1)*exp(r*(1-N1(i-1,1))));
33
34             %Ring Y
35             N2(i,n)=b*(N2(i-1,n-1)*exp(r*(1-N2(i-1,n-1))))...
36                 +a*(N2(i-1,n)*exp(r*(1-N2(i-1,n))))...
37                 +b*(N2(i-1,1)*exp(r*(1-N2(i-1,1))));

```

```

38     else
39         %Ring X
40         N1(i,j)=b*(N1(i-1,j-1)*exp(r*(1-N1(i-1,j-1))))...
41             +a*(N1(i-1,j)*exp(r*(1-N1(i-1,j))))...
42             +b*(N1(i-1,j+1)*exp(r*(1-N1(i-1,j+1))));
43
44         %Ring Y
45         N2(i,j)=b*(N2(i-1,j-1)*exp(r*(1-N2(i-1,j-1))))...
46             +a*(N2(i-1,j)*exp(r*(1-N2(i-1,j))))...
47             +b*(N2(i-1,j+1)*exp(r*(1-N2(i-1,j+1))));
48     end
49 end
50 end
51 N = [N1 N2];

```


Listing A.13: Figure 6.1: Coupled tangent map

```

1 function [ tanmap ] = tanmap_ricker_nearestNeighbor_coupled ( Ni, b, r, n, c, k, ...
    1 )
2 a = 1-2*b;           % Initial conditions
3 l = 1 + n;
4 tanmap=zeros(2*n);
5 for i=1:2*n          % Tangent map
6     if i==1
7         tanmap(1,n)=b*(exp(r*(1-Ni(n)))*(1-r*Ni(n)));
8         tanmap(1,1)=a*(exp(r*(1-Ni(1)))*(1-r*Ni(1)));
9         tanmap(1,2)=b*(exp(r*(1-Ni(2)))*(1-r*Ni(2)));
10    elseif i==n
11        tanmap(n,n-1)=b*(exp(r*(1-Ni(n-1)))*(1-r*Ni(n-1)));
12        tanmap(n,n)=a*(exp(r*(1-Ni(n)))*(1-r*Ni(n)));
13        tanmap(n,1)=b*(exp(r*(1-Ni(1)))*(1-r*Ni(1)));
14    elseif i==n+1
15        tanmap(n+1,2*n)=b*(exp(r*(1-Ni(2*n)))*(1-r*Ni(2*n)));
16        tanmap(n+1,n+1)=a*(exp(r*(1-Ni(n+1)))*(1-r*Ni(n+1)));
17        tanmap(n+1,n+2)=b*(exp(r*(1-Ni(n+2)))*(1-r*Ni(n+2)));
18    elseif i==2*n
19        tanmap(2*n,2*n-1)=b*(exp(r*(1-Ni(2*n-1)))*(1-r*Ni(2*n-1)));
20        tanmap(2*n,2*n)=a*(exp(r*(1-Ni(2*n)))*(1-r*Ni(2*n)));
21        tanmap(2*n,n+1)=b*(exp(r*(1-Ni(n+1)))*(1-r*Ni(n+1)));
22    else
23        tanmap(i,i-1)=b*(exp(r*(1-Ni(i-1)))*(1-r*Ni(i-1)));
24        tanmap(i,i)=a*(exp(r*(1-Ni(i)))*(1-r*Ni(i)));
25        tanmap(i,i+1)=b*(exp(r*(1-Ni(i+1)))*(1-r*Ni(i+1)));
26    end
27 end
28 %% Connecting coupled nodes
29
30 tanmap(k,l)=c*(exp(r*(1-Ni(k)))*(1-r*Ni(k)));
31 tanmap(l,k)=c*(exp(r*(1-Ni(l)))*(1-r*Ni(l)));

```

Listing A.14: Figure 6.3

```
1  %Initial Conditions
2  map='map-ricker.nearestNeighbor-coupled';
3  tanmap='tanmap-ricker.nearestNeighbor-coupled';
4  iteration=2000000;
5  lce_iteration=50000;
6  b=0.2;
7  r=3; %unused in this case
8  n=32; %nodes
9  s=1; %seed
10
11 %Find LCEs
12 LCEvector = LCE ( map, tanmap, iteration, lce_iteration, b, r, n, s );
13
14 figure(2)
15 plot((1:64)', LCEvector, '.')
16 xlabel('LCE number')
17 ylabel('LCEs')
```

Listing A.15: Figure 6.5(a): Coupled nonhomogeneous map

```

1 function [ N ] = map_ricker_nearestNeighbor_coupled_nonhom_quad1to1 ( iteration, ...
    b, r, n, s, c )
2 % Initial conditions for first X
3 N1=zeros(iteration, n);
4 rand('seed', s)
5 N1(1,:) = rand(1,n)+.5;
6
7 % Initial conditions for second Y
8 s = s+1;
9 N2=zeros(iteration, n);
10 rand('seed', s)
11 N2(1,:) = rand(1,n)+.5;
12
13 a=1-2*b;
14
15 for i=2:iteration      % Map of Ricker connecting to nearest neighbor
16     for j=1:n
17
18         %Nonhomogeneous ring
19         if j≤24
20             r=3;
21         else
22             r=4.6;
23         end
24
25         %Connecting nodes 2-6 on ring X to nodes 3-6 on ring Y, respectively
26         if j≥3 && j≤6
27             c=0.65;
28         else
29             c=0;
30         end
31
32         if j==1
33             %Ring X
34             N1(i,1)=b*(N1(i-1,n)*exp(r*(1-N1(i-1,n))))...
35                 +a*(N1(i-1,1)*exp(r*(1-N1(i-1,1))))...
36                 +b*(N1(i-1,2)*exp(r*(1-N1(i-1,2))));

```

```

37
38         %Ring Y
39         N2(i,1)=b*(N2(i-1,n)*exp(r*(1-N2(i-1,n))))...
40             +a*(N2(i-1,1)*exp(r*(1-N2(i-1,1))))...
41             +b*(N2(i-1,2)*exp(r*(1-N2(i-1,2))));
42
43     elseif j==n
44         %Ring X
45         N1(i,n)=b*(N1(i-1,n-1)*exp(r*(1-N1(i-1,n-1))))...
46             +a*(N1(i-1,n)*exp(r*(1-N1(i-1,n))))...
47             +b*(N1(i-1,1)*exp(r*(1-N1(i-1,1))));
48
49         %Ring Y
50         N2(i,n)=b*(N2(i-1,n-1)*exp(r*(1-N2(i-1,n-1))))...
51             +a*(N2(i-1,n)*exp(r*(1-N2(i-1,n))))...
52             +b*(N2(i-1,1)*exp(r*(1-N2(i-1,1))));
53     else
54         %Ring X
55         N1(i,j)=b*(N1(i-1,j-1)*exp(r*(1-N1(i-1,j-1))))...
56             +a*(N1(i-1,j)*exp(r*(1-N1(i-1,j))))...
57             +b*(N1(i-1,j+1)*exp(r*(1-N1(i-1,j+1))))...
58             +c*(N2(i-1,j)*exp(r*(1-N2(i-1,j))));
59
60         %Ring Y
61         N2(i,j)=b*(N2(i-1,j-1)*exp(r*(1-N2(i-1,j-1))))...
62             +a*(N2(i-1,j)*exp(r*(1-N2(i-1,j))))...
63             +b*(N2(i-1,j+1)*exp(r*(1-N2(i-1,j+1))))...
64             +c*(N1(i-1,j)*exp(r*(1-N1(i-1,j))));
65     end
66 end
67 end
68 N = [N1 N2];

```

Listing A.16: Figure 6.5(a): Coupled nonhomogeneous tangent map

```

1 function [ tanmap ] = tanmap_ricker_nearestNeighbor_coupled_nonhom_quad1to1 ( ...
    Ni, b, r, n, c, k, l )
2 a = 1-2*b;           % Initial conditions
3 l = l + n;
4 tanmap=zeros(2*n);
5 for i=1:2*n          % Tangent map
6
7     if i≤24
8         r=3;
9     else
10        r=4.6;
11    end
12
13    if i==1
14        tanmap(1,n)=b*(exp(r*(1-Ni(n)))*(1-r*Ni(n)));
15        tanmap(1,1)=a*(exp(r*(1-Ni(1)))*(1-r*Ni(1)));
16        tanmap(1,2)=b*(exp(r*(1-Ni(2)))*(1-r*Ni(2)));
17    elseif i==n
18        tanmap(n,n-1)=b*(exp(r*(1-Ni(n-1)))*(1-r*Ni(n-1)));
19        tanmap(n,n)=a*(exp(r*(1-Ni(n)))*(1-r*Ni(n)));
20        tanmap(n,1)=b*(exp(r*(1-Ni(1)))*(1-r*Ni(1)));
21    elseif i==n+1
22        tanmap(n+1,2*n)=b*(exp(r*(1-Ni(2*n)))*(1-r*Ni(2*n)));
23        tanmap(n+1,n+1)=a*(exp(r*(1-Ni(n+1)))*(1-r*Ni(n+1)));
24        tanmap(n+1,n+2)=b*(exp(r*(1-Ni(n+2)))*(1-r*Ni(n+2)));
25    elseif i==2*n
26        tanmap(2*n,2*n-1)=b*(exp(r*(1-Ni(2*n-1)))*(1-r*Ni(2*n-1)));
27        tanmap(2*n,2*n)=a*(exp(r*(1-Ni(2*n)))*(1-r*Ni(2*n)));
28        tanmap(2*n,n+1)=b*(exp(r*(1-Ni(n+1)))*(1-r*Ni(n+1)));
29    else
30        tanmap(i,i-1)=b*(exp(r*(1-Ni(i-1)))*(1-r*Ni(i-1)));
31        tanmap(i,i)=a*(exp(r*(1-Ni(i)))*(1-r*Ni(i)));
32        tanmap(i,i+1)=b*(exp(r*(1-Ni(i+1)))*(1-r*Ni(i+1)));
33    end
34 end
35
36 %% Connecting coupled nodes

```

```
37
38 for i = 1:length(k)
39     tanmap(k(i),l(i))=c*(exp(r*(1-Ni(k(i))))*(1-r*Ni(k(i))));
40     tanmap(l(i),k(i))=c*(exp(r*(1-Ni(l(i))))*(1-r*Ni(l(i))));
41 end
42
43 end
```

Listing A.17: Figure 6.5(b)

```

1  %% fig a: time evolution
2  % x12
3  iteration=2000050;
4  b=0.2;
5  r=3;
6  n=32; %nodes
7  s=1; %seed
8  N.span=50; %frame of plot
9  node = 12;
10 c = 0.65;
11
12 [ N ] = map_ricker_nearestNeighbor_coupled_nonhom_quad4to4 ( iteration, b, r, n, ...
    s, c );
13
14 figure(1)
15 subplot(2,2,1), plot(iteration-N.span:iteration, ...
    N(iteration-N.span:iteration,node), '*', 'color', 'black')
16 hold on;
17
18 %x27
19 iteration=2000050;
20 b=0.2;
21 r=3;
22 n=32; %nodes
23 s=1; %seed
24 N.span=50; %frame of plot
25 node = 27;
26 c = 0.65;
27
28 [ N ] = map_ricker_nearestNeighbor_coupled_nonhom_quad4to4 ( iteration, b, r, n, ...
    s, c );
29
30 subplot(2,2,1), plot(iteration-N.span:iteration, ...
    N(iteration-N.span:iteration,node), 'o', 'color', 'black')
31 xlabel('Iteration number')
32 ylabel('N')
33 legend('x-12', 'x-27')

```

```

34
35 %% fig b: LCE Number
36 map='map_ricker.nearestNeighbor.coupled.nonhom.quad4to4';
37 tanmap='tanmap_ricker.nearestNeighbor.coupled.nonhom.quad4to4';
38 iteration=2000;
39 lce_iteration=50;
40 b=0.2;
41 r=3; %unused in this case
42 n=32; %nodes
43 s=1; %seed
44 k=[27 28 29 30];
45 l=[27 28 29 30];
46 c=0.65;
47
48 %Find LCEs
49 LCEvector = LCE_coupled ( map, tanmap, iteration, lce_iteration, b, r, n, s, c, ...
    k, l );
50
51 subplot(2,2,2), plot((1:64)', LCEvector, 'black.')
52 xlabel('LCE number')
53 ylabel('LCEs')
54
55 %% Fig c: Time delay x12
56 iteration=2000050;
57 b=0.2;
58 r=3;
59 n=32; %nodes
60 s=1; %seed
61 N_span=50; %frame of plot
62 node = 12;
63 c = 0.65;
64
65 N = map_ricker.nearestNeighbor.coupled.nonhom.quad4to4 ( iteration, b, r, n, s, ...
    c );
66
67 N1 = N(:, node);
68
69 x_t      = N1(iteration-49: iteration);

```



```

70 x_t_minus_1 = N1(iteration-50: iteration-1);
71 x_t_minus_2 = N1(iteration-51: iteration-2);
72 T = table(x_t, x_t_minus_1, x_t_minus_2);
73
74 subplot(2,2,3), plot3(x_t, x_t_minus_1, x_t_minus_2, 'black. ');
75 grid on
76 xlabel('x_{12}(t)')
77 ylabel('x_{12}(t-1)')
78 zlabel('x_{12}(t-2)')
79
80 %% Fig c: Time delay x27
81 iteration=2000050;
82 b=0.2;
83 r=3;
84 n=32; %nodes
85 s=1; %seed
86 N_span=50; %frame of plot
87 node = 27;
88 c = 0.65;
89
90 N = map_ricker_nearestNeighbor_coupled_nonhom_quad4to4 ( iteration, b, r, n, s, ...
      c );
91
92 N1 = N(:, node);
93
94 x_t      = N1(iteration-49: iteration);
95 x_t_minus_1 = N1(iteration-50: iteration-1);
96 x_t_minus_2 = N1(iteration-51: iteration-2);
97
98
99 T = table(x_t, x_t_minus_1, x_t_minus_2);
100
101 subplot(2,2,4), plot3(x_t, x_t_minus_1, x_t_minus_2, 'black. ');
102 grid on
103 xlabel('x_{27}(t)')
104 ylabel('x_{27}(t-1)')
105 zlabel('x_{27}(t-2)')

```